Structural Diversity of Sulfide Complexes Containing Half-Sandwich Cp*Ta and Cp*Nb Fragments

Kazuyuki Tatsumi,*,† Yoshihisa Inoue,‡ Hiroyuki Kawaguchi,† Masaki Kohsaka,‡ Akira Nakamura,*,‡ Roger E. Cramer,*,§ William VanDoorne,§ Ginger J. Taogoshi,§ and Paul N. Richmann§

Department of Chemistry, Faculty of Engineering Science, Osaka University, Toyonaka, Osaka 560, Japan, Department of Macromolecular Science, Faculty of Science, Osaka University, Toyonaka, Osaka 560, Japan, and Department of Chemistry, University of Hawaii, Honolulu, Hawaii 96822

Received July 21, 1992

The disulfide (S_2^{2-}) complex $Li_2(thf)_3[Cp^*Ta(S_2)(\mu\text{-}S_2)]_2(\mu\text{-}O)$ (**4**) was isolated from the reaction of $[Cp^*TaCl_3]_2(\mu\text{-}O)$ and 4 equiv of Li_2S_x (x = 2–5) in THF. In contrast, reaction of Cp^*MCl_4 (M = Ta, Nb) and 4–5 equiv of Li_2S_2 afforded the sulfide complexes $[Li_2(thf)_2Cp^*MS_3]_2$ (M = Ta (**5a**), Nb (**5b**)), containing the unique organometallic $Cp^*MS_3^{2-}$ unit carrying three terminal sulfides, whose dimers comprise a $Li_4M_2S_6$ hexagonal prismatic core. The THF molecules coordinated at Li in **5a** can be readily replaced by DME and TMEDA to give $[Li_2(dme)Cp^*TaS_3]_2$ (**6**) and $Li_2(tmeda)_2Cp^*TaS_3$ (**7**), respectively. When the reaction between Cp^*TaCl_4 and 4–5 equiv of Li_2S_2 was carried out in the presence of excess TMEDA, LiCl was incorporated into the cluster, and $[Li_3(tmeda)_2Cp^*TaS_3Cl]_2(\mu\text{-tmeda})$ (**8**) was isolated. The Li_3TaS_3Cl core of **8** has an open-cubane geometry, and two such units are joined by a bridging TMEDA molecule. The room-temperature ^1H NMR of **8** in C_6D_6 shows a single set of TMEDA resonances, indicating that ligand-exchange processes between chelating TMEDA ligands and between chelating TMEDA and bridging TMEDA are very fast. Treatment of Cp^*TaCl_4 with 4–5 equiv of Li_2S gave $Li_2(thf)_2Cp^*_3Ta_3S_6$ (**9**) in addition to **5a**. Thus partial reduction of tantalum occurred under these conditions, leading to the formation of a triangular $Ta^{IV}_2Ta^V$ frame in **9**. All the isolated clusters reported here contain lithiums which are strongly bound to sulfurs and/or oxygen (for **4**). The X-ray-derived structures of **4**, **5a**, and **8** are described in detail. Crystal data are as follows. For $Li_2(thf)_3[Cp^*Ta(S_2)(\mu\text{-}S_2)]_2(\mu\text{-}O)\cdot THF$ (**4**): monoclinic, space group = $P2_1/n$, a = 17.81 (2) Å, b = 13.000 (9) Å, c = 19.96 (2) Å, β = 95.91 (7)°, Z = 4, V = 4598 (6) Å^3. For $[Li_2(thf)_2Cp^*TaS_3]_2$ (**5a**): monoclinic, space group = $C2/c$, a = 24.879 (5) Å, b = 11.501 (2) Å, c = 16.669 (3) Å, β = 99.21 (1)°, Z = 4, V = 4709 (1) Å^3. For $[Li_3(tmeda)_2Cp^*TaS_3Cl]_2(\mu\text{-tmeda})$ (**8**): triclinic, space group = $P\bar{1}$, a = 10.902 (4) Å, b = 11.169 (3) Å, c = 17.154 (5) Å, α = 83.06 (2), β = 88.43 (3)°, γ = 64.00 (2)°, Z = 1, V = 1863 (1) Å^3.

Introduction

Soluble transition-metal sulfides represent one of the most fruitful specialities in coordination chemistry, in view of their structural and electrochemical diversity. The significance of sulfide complexes is also well-established in the area of transition-metal clusters and metalloenzymatic catalyses.[1] An important class of metal sulfides is those containing cyclopentadienyls,[2] where introduction of the organic auxiliary ligands often promotes solubility of metal sulfides and thereby makes their chemistry tractable.

Our interest in sulfide chemistry of pentamethylcyclopentadienyl tantalum, Cp*Ta (Cp* = C_5Me_5), was stimulated by the EI mass fragmentation patterns of the bis(dithiolato) complexes, $Cp^*Ta(SCH{=}CHS)_2$ (**1**), $Cp^*Ta(SCH_2CH_2S)_2$ (**2**),[3] and $Cp^*Ta(ndt)_2$ (**3**; ndt = norbornane-*exo*-2,3-dithiolate).[4] As schematically shown in Scheme I, the mass spectra exhibit peaks associated with the mono- and bis(disulfido(2–)) complex cations along with the parent ion isotopic clusters. These fragment ions are presumably formed by a loss of one or two olefin moieties from the dithiolate ligands, while for **1** the first fragmentation step involves liberation of "SH", thus generating an intriguing SC_2H or C_2SH group.[5]

Our attempts to chemically synthesize relevant disulfido(2–) complexes from reactions of $(Cp^*TaCl_3)_2(\mu\text{-}O)$, Cp^*TaCl_4, and Cp^*NbCl_4 with Li_2S_x (x = 1, 2, 5) resulted in the formation of a series of new tantalum and niobium sulfides that include $Li_2(thf)_3[Cp^*Ta(S_2)(\mu\text{-}S_2)]_2(\mu\text{-}O)$ (**4**),

† Department of Chemistry, Osaka University.
‡ Department of Macromolecular Science, Osaka University.
§ Department of Chemistry, University of Hawaii.

(1) (a) Holm, R. H. *Acc. Chem. Res.* **1977**, *10*, 427–434. (b) Müller, A.; Diemann, E.; Jostes, R.; Bögge, H. *Angew. Chem., Int. Ed. Engl.* **1981**, *20*, 934–955. (c) Coucouvanis, D. *Acc. Chem. Res.* **1981**, *14*, 201–209. (d) Draganjac, M.; Rauchfuss, T. B. *Angew. Chem., Int. Ed. Engl.* **1985**, *24*, 742–757. (e) Fenske, D.; Ohmer, J.; Hachgenei, J.; Merzweiler, K. *Angew. Chem., Int. Ed. Engl.* **1988**, *27*, 1277–1296. (f) Lee, S. C.; Holm, R. H. *Angew Chem., Int. Ed. Engl.* **1990**, *29*, 840–856.

(2) (a) Casewit, C. J.; Rakowski DuBois, M. *J. Am. Chem. Soc.* **1986**, *108*, 5482–5489 and references therein. (b) Beck, W.; Danzer, W.; Thiel, G. *Angew Chem., Int. Ed. Engl.* **1973**, *12*, 582–583. (c) Bolinger, C. M.; Rauchfuss, T. B.; Wilson, S. R. *J. Am. Chem. Soc.* **1982**, *104*, 7313–7314. (d) Zank, G. A.; Jones, C. A.; Rauchfuss, T. B.; Rheingold, A. L. *Inorg. Chem.* **1986**, *25*, 1886–1891. (e) Brunner, H.; Meier, W.; Wachter, J.; Guggoltz, E.; Zahn, T.; Ziegler, M. L. *Organometallics* **1982**, *1*, 1107–1113. (f) Brunner, H.; Wachter, J.; Guggolz, E.; Ziegler, M. L. *J. Am. Chem. Soc.* **1982**, *104*, 1765–1766. (g) Brunner, H.; Klement, Wachter, J.; Tsunoda, M.; Leblanc, J.-C.; Moise, C. *Inorg. Chem.* **1990**, *29*, 584–585. (h) Rakowski Dubois, M. *Chem. Rev.* **1989**, *89*, 1–9. (i) Wachter, J. *Angew. Chem., Int. Ed. Engl.* **1989**, *28*, 1613–1626.

(3) Tatsumi, K.; Takeda, J.; Sekiguchi, Y.; Kohsaka, M.; Nakamura, A. *Angew. Chem., Int. Ed. Engl.* **1985**, *24*, 332–333.

(4) Tatsumi, K.; Inoue, Y.; Nakamura, A. *J. Organomet. Chem.*, in press.

(5) The unusual EI fragmentation of **1** indicates the presence of significant bonding interactions between Ta and the olefin carbons. See ref 3.

0276-7333/93/2312-0352$04.00/0

Scheme I. EI Mass Fragmentation Patterns

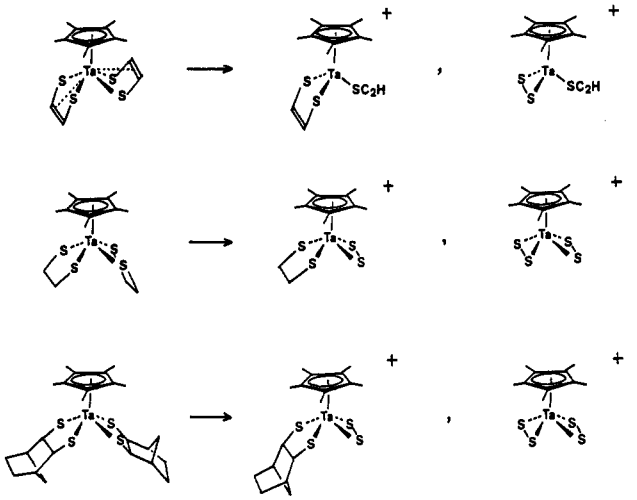

$[Li_2(thf)_2Cp^*MS_3]_2$ (M = Ta (**5a**), Nb (**5b**)), $[Li_2(dme)Cp^*TaS_3]_2$ (**6**), $Li_2(tmeda)_2Cp^*TaS_3$ (**7**), $[Li_3(tmeda)_2Cp^*TaS_3Cl]_2(\mu$-tmeda) (**8**), and $Li_2(thf)_2Cp^*_3Ta_3S_6$ (**9**). This paper describes syntheses of these tantalum and niobium sulfides and the X-ray structure analysis of **4**, **5a**, and **8**. The nature of the Ta=S bonds in the $Cp^*TaS_3^{2-}$ unit is discussed with the aid of a molecular orbital analysis. A preliminary account concerning **5a** has been reported.[6]

The expected $Cp^*Ta(S_2)_2$ moieties (A) are in fact present in the structure of **4**, where two S_2 units and an oxygen atom bridge two such units. In contrast, when the μ-O

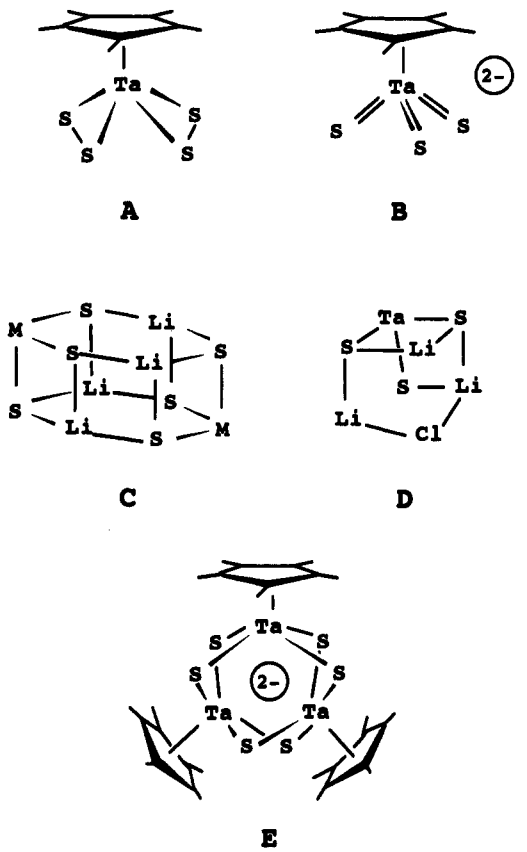

bridge is absent, the Cp*Ta and Cp*Nb fragments tend to accommodate three monosulfides (S^{2-}), instead of two disulfides (S_2^{2-}), thus forming the novel $Cp^*Ta(S)_3^{2-}$ unit (B). In the case of **5a**, and **5b**, four Li cations link two Cp*M (M = Ta, Nb) units to give a hexagonal prismatic $Li_4M_2S_6$ cluster (C), while for **8** LiCl is incorporated into the $Li_2Cp^*TaS_3$ structure leading to an open-cubane Li_3TaS_3Cl frame (D), yet another intriguing cluster structure. Furthermore, when Cp^*TaCl_4 was reacted with Li_2S, a partial reduction of Ta occurs, resulting in formation of a mixed-valence $Cp^*_3Ta_3S_6^{2-}$ cluster (E) with a triangular $Ta^{IV}_2Ta^V$ frame. Interestingly regardless of the stoichiometry of the lithium sulfides used, the isolated products are the disulfido(2–) or the monosulfido complexes, and formation of larger polysulfido–metal rings, MS_x ($x > 2$), was not noticed.

Our synthetic study of **4**–**9** provides a new convenient entry into rare Ta sulfides. Another important aspect is that lithiums are not innocent countercations, but they are strongly coordinated at sulfurs, thus participating in formation of the stable cluster structures. Having lithium cations, the $Cp^*TaS_3^{2-}$ and $Cp^*_3Ta_3S_6^{2-}$ units could serve as potential building blocks of a wide range of homo- and heteronuclear sulfide clusters.[7]

Experimental Section

All operations and manipulations were carried out under an argon atmosphere using standard Schlenk techniques. Reagent grade THF, toluene, benzene, hexane, ether, and DME (1,2-dimethoxyethane) were deoxygenated and dried by reflux over sodium benzophenone and were distilled under argon before use. TMEDA (*N,N,N',N'*-tetramethylethylenediamine) and deuterated solvents were trap-to-trap distilled from calcium hydride or sodium. Cp^*MCl_4 (M = Ta, Nb) were prepared from $Cp^*(SnBu_3)$ or $Cp^*(SiMe_3)$ and MCl_5 in toluene.[8]

^{1}H NMR spectra were recorded on JEOL FX-100, GSX-270, and GSX-400 spectrometers, and the data are listed in ppm downfield from TMS. For UV–visible spectra, JASCO UNIDEV-500 and U-best-30 spectrometers were used. IR spectra were measured on a JASCO DS-402G spectrometer, while Raman spectra were obtained on a JASCO R-800 spectrometer equipped with an NEC GLG 5800 He–Ne laser.

Preparation of Li_2S_x (x = 1, 2, and 5). Water-free "Li_2S_2" was synthesized by reaction of lithium metal with elemental sulfur, S_8, ($1:{}^1/_8$) in liquid ammonia. This "Li_2S_2" was nearly identical with that prepared from the reaction between $LiEt_3BH$ (Super Hydride) and ${}^1/_8S_8$[9] according to their Raman spectra. Before use, the resulting fine yellow powder was occasionally washed a few times with THF under Ar until the filtrate became nearly colorless. Likewise, "Li_2S_5" and "Li_2S" were prepared as orange and fine white powders, respectively, from the $1:{}^5/_{16}$ and $1:{}^1/_{16}$ Li/S_8 reaction systems in liquid ammonia. These lithium sulfides are highly hygroscopic.

Preparation of $Li_2(thf)_3[Cp^*Ta(S_2)(\mu\text{-}S_2)]_2(\mu\text{-}O)\cdot THF$ (4). The starting binuclear halide complex, $(Cp^*TaCl_3)_2(\mu$-O), was prepared in situ and was used without further purification.[10] Thus, 3 equiv of water (0.10 g, 0.6 mmol) in THF (3.3 mL) was added to a THF solution (15 mL) of Cp^*TaCl_4 (0.97 g, 2.1 mmol) at room temperature. The color of the solution turned immediately from deep red to light yellow. After stirring for 1 h, the

(6) Tatsumi, K.; Inoue, Y.; Nakamura, A.; Cramer, R. E.; VanDoorne, W.; Gilje, J. W. *J. Am. Chem. Soc.* **1989**, *111*, 782–783.

(7) We have confirmed that the $Cp^*TaS_3Li_2$ species react readily with $[Rh(COD)Cl]_2$, $RuH(Cl)(PPh_3)_3$, etc. to generate mixed metal clusters. The results will be published separately.

(8) (a) Sanner, R. D.; Cater, S. T.; Bruton, W. J., Jr. *J. Organomet. Chem.* **1982**, *240*, 157–162. (b) Okamoto, T.; Yasuda, H.; Nakamura, A.; Kai, Y.; Kanehisa, N.; Kasai, N. *J. Am. Chem. Soc.* **1988**, *110*, 5008–5017.

(9) (a) Gladysz, J. A.; Wong, V. K.; Jick, B. S. *Tetrahedron* **1978**, *35*, 2329–2335. (b) Letoffe, J. M.; Thourey, J.; Perachon, G.; Bousequet, J. *Bull Soc. Chim. Fr.* **1976**, 424–426. (c) Dubois, P.; Lelieur, J. P.; Lepoutre, G. *Inorg. Chem.* **1988**, *27*, 73–80.

(10) Jernakoff, P.; Bellefon, C. M.; Geoffroy, G. L.; Rheingold, A. L.; Geib, S. T. *Organometallics* **1987**, *6*, 1362–1364.

solvent was evaporated to dryness to give $(Cp^*TaCl_3)_2(\mu\text{-}O)$ as a yellow solid which was then dissolved in dry THF (15 mL). The resulting yellow solution was added to a slurry of Li_2S_2 (0.39 g, 5.1 mmol) in THF (15 mL). The reaction mixture was stirred for 1 h, during which time the color of the solution became red. After removal of the solvent, the residue was extracted with benzene (2 × 30 mL). The extracts were filtered and dried in vacuo, and the yellow solid obtained therefrom was recrystallized from THF to give 0.36 g (0.32 mmol) of **4** as yellow crystals (30% overall yield based on Ta). Mp: 140 °C dec. ^{1}H NMR (100 MHz, C_6D_6): δ 2.10 (s, 30 H, Cp*), 3.60 (m, 12 H, thf), 1.40 (m, 12 H, thf). ^{1}H NMR (270 MHz, THF-d_8): δ 1.95 (s, Cp*). Far IR (KBr, Nujol): 585 (s), 512 (m), 336 (s) cm^{-1}. Raman: 614 (w), 604 (s), 550 (m), 517 (s), 406 (m), 331 (s) cm^{-1}. Anal. Calcd for $C_{32}H_{54}O_4S_8Li_2Ta_2$: C, 33.86; H, 4.80; S, 22.60. Found: C, 33.55; H, 4.64; S, 22.92.

Preparation of $[Li_2(thf)_2Cp^*TaS_3]_2$ (5a). To a slurry of Li_2S_2 (1.9 g, 24 mmol) in THF (30 mL) was added a solution of Cp^*TaCl_4 (1.8 g, 3.9 mmol) in THF (20 mL) at 0 °C. The color of the solution turned from red to yellow. The reaction mixture was stirred at room temperature for 2 h, and then the solution was filtered to remove insoluble materials. After evaporation, the resulting yellow oily material was extracted with benzene (2 × 60 mL). The orange solution was filtered and dried in vacuo. Recrystallization of the yellow solid from THF/hexane (1:2) gave 0.68 g (0.60 mmol) of **5a** as light yellow crystals (31% yield). Note that pure crystals of **5a** are hardly soluble in benzene, although the extraction of the crude oily product was best made with benzene. ^{1}H NMR (400 MHz, THF-d_8): δ 2.03 (s, Cp*). Raman: 619 (w), 597 (m), 552 (w), 434 (s), 418 (sh), 368 (w), 354 (w) cm^{-1}. UV–visible (λ_{max}, nm (ε × 10^{-3}, M^{-1} cm^{-1}), THF): 302 (16.6). Anal. Calcd for $C_{36}H_{62}O_4S_6Li_4Ta_2$: C, 37.90; H, 5.48; S, 16.86. Found: C, 34.48; H, 5.36; S, 16.56. The observed carbon contents are systematically lower than the calculated values for **5a**, **7**, and **8**, because of the hygroscopic nature of the complexes.

Preparation of $[Li_2(thf)_2Cp^*NbS_3]_2$ (5b). The reaction between Cp^*NbCl_4 (0.96 g, 2.6 mmol) and Li_2S_2 (1.4 g, 18 mmol) in THF followed by a workup similar to that of the Ta analog **5a** gave 50 mg (0.052 mmol) of **5b** as yellow crystals (4% yield). ^{1}H NMR (100 MHz, THF-d_8): δ 2.00 (s, Cp*). Raman: 622 (w), 598 (w), 433 (s), 409 (w), 363 (m) cm^{-1}. UV–visible (λ_{max}, nm (ε × 10^{-3}, M^{-1} cm^{-1}), THF): 341 (14.0).

Reaction of 5a with DME. **5a** (0.06 g, 0.05 mol) was dissolved in DME (10 mL), and the solution was stirred at room temperature for 15 min. The sample was concentrated in vacuo to ca. 1 mL, to which 1 mL of hexane was added. Upon overnight standing at −20 °C, light yellow needles formulated as $Li_2(dme)Cp^*TaS_3$ (**6**) were formed. By ^{1}H NMR criteria the conversion of **5a** into **6** occurs nearly stoichiometrically. Like **5a**, the crystals of **6** are hardly soluble in benzene but dissolve well in THF and CH_3CN. ^{1}H NMR (270 MHz, CD_3CN): δ 2.08 (s, 15 H, Cp*), 3.26 (s, 6 H, dme (CH_3)), 3.43 (s, 4 H, dme (CH_2)). Raman: 618 (w), 596 (m), 555 (w), 432 (s), 414 (m), 402 (sh), 351 (w), cm^{-1}. UV–visible (λ_{max}, nm (ε × 10^{-3}, M^{-1} cm^{-1}), DME): 305 (6.5). Anal. Calcd for $C_{14}H_{25}O_2S_3Li_2Ta$: C, 32.56; H, 4.88, S, 18.63. Found: C, 32.54; H, 4.47; S, 18.00. Complex **6** is most hygroscopic among the sulfide complexes reported here, and the elemental analysis was performed by sealing the sample in a thin aluminum tube.

Reaction of 5a with TMEDA. To a suspension of **5a** (0.10 g, 0.09 mmol) in toluene (6 mL) was added an excess of TMEDA (0.50 mL, 3.3 mmol) at room temperature. The reaction mixture immediately turned into a homogeneous yellow solution. After stirring for 30 min, the solution was concentrated to ca. 1 mL and was stored at −20 °C. Light yellow microcrystals formulated as $Li_2(tmeda)_2Cp^*TaS_3$ (**7**) were then obtained. By ^{1}H NMR criteria, the conversion of **5a** into **7** is nearly stoichiometric. In contrast to **5a** and **6**, crystals of **7** are soluble in benzene. ^{1}H NMR (270 MHz, C_6D_6): δ 2.14 (s, 8 H, tmeda (CH_2)), 2.42 (s, 24 H, tmeda (CH_3)), 2.45 (s, 15 H, Cp*). Raman: 618 (w), 595 (m), 552 (w), 432 (s), 424 (sh), 402 (m), 348 (w) cm^{-1}. UV–visible (λ_{max}, nm (ε × 10^{-3}, M^{-1} cm^{-1}), benzene): 305 (6.0). Anal. Calcd for $C_{22}H_{47}N_4S_3Li_2Ta$: C, 40.12; H, 7.19; N, 8.51; S, 14.60. Found: C, 36.04; H, 7.10; N, 7.68; S, 13.99.

Preparation of $[Li_3(tmeda)_2Cp^*TaS_3Cl]_2(\mu\text{-tmeda})$ (8). A THF solution (20 mL) of Cp^*TaCl_4 (2.3 g, 5.0 mmol) was added to a slurry of Li_2S_2 (2.1 g, 27 mmol) in THF (30 mL) at 0 °C. The reaction mixture was stirred at room temperature for 2 h, and the solvent was removed in vacuo. The oily residue was extracted with benzene (60 mL)/TMEDA (5.0 mL, 33 mmol). The orange-red solution was filtered, dried in vacuo, and the resulting orange solid was dissolved in THF (20 mL). After adding 40 mL of hexane, the solution was concentrated to ca. 10 mL, and stored overnight at −20 °C. Light yellow crystals of **8** (2.0 g, 1.3 mmol) precipitated (53% yield) along with orange crystals of $Li_2S_6(tmeda)_2$.[11] Since the crystals of $Li_2S_6(tmeda)_2$ are relatively large in size and the color clearly differs, manual separation from **8** was possible. The crystals of **8** are soluble in benzene, but to a lesser degree than **7**. ^{1}H NMR (270 MHz, C_6D_6): δ 2.24 (s, 20 H, tmeda(CH_2)), 2.30 (s, 60 H, tmeda(CH_3)), 2.43 (s, 30 H, Cp*). Raman: 618 (w), 595 (m), 552 (w), 453 (s), 418 (s), 402 (sh), 350 (m) cm^{-1}. UV–visible (λ_{max}, nm (ε × 10^{-3}, M^{-1} cm^{-1}), THF): 301 (20.5). Anal. Calcd for $C_{50}H_{110}N_{10}S_6Cl_2Li_6Ta_2$: C, 39.55; H, 7.30; N, 9.23; S, 12.67. Found: C, 36.17; H, 7.15; N, 7.67; S, 12.91.

Reaction of 7 with LiCl. to a slurry of LiCl (10 mg, 0.24 mmol) in benzene were added TMEDA (0.2, 1.3 mmol) and a benzene solution (5 mL) of **7** (40 mg, 0.06 mmol). After stirring 1 h, the solvent and unreacted TMEDA were evaporated in vacuo to give a light yellow crystalline powder. According to its ^{1}H NMR spectrum, the product is **8**, in a nearly pure form.

Reaction of Cp^*TaCl_4 with Li_2S. Upon adding a THF solution (20 mL) of Cp^*TaCl_4 (1.4 g, 2.9 mmol) to a slurry of Li_2S (0.65 g, 14.1 mmol) in THF (10 mL) at 0 °C, the color of the solution became dark red. After stirring for 2 h, the solvent was evaporated to dryness to give a red oily residue. A workup similar to the one described for the synthesis of **5a** and recrystallization from THF gave first dark red crystals and then light yellow crystals. The latter light yellow crystals were characterized unequivocally as **5a**. According to the preliminary X-ray structure analysis, the red complex **9** was formulated as $Cp^*_3Ta_3S_6Li_2(thf)_2$. The isolated yields as crystals of **5a** and **9** are 7% (0.12 g) and 21% (0.27 g), respectively. UV–visible (**9**) (λ_{max}, nm (ε × 10^{-3}, M^{-1} cm^{-1}), THF): 285 (11), 309 (8.5), 356 (13), 515 (1.2), 701 (0.22).

X-ray Crystallographic Study of 4. A crystal (0.7 × 0.7 × 0.6 mm) of $Li_2(thf)_3[Cp^*Ta(S_2)_2]_2(\mu\text{-}O)\cdot THF$ obtained from the preparation described above was sealed carefully in a thin-walled glass capillary under a THF/Ar atmosphere. The compound is rather stable as a solid in the air, but its crystal form is rapidly destroyed in the absence of a THF solvent. Thus it is necessary to handle the crystals under a THF atmosphere.

A Rigaku AFC5R diffractometer operating at ambient temperature was used to collect the diffraction data, with graphite-monochromated Mo Kα radiation (α = 710 69 Å). The unit cell constants were first determined by least-squares analysis of the centered angular coordinates of 14 independent intense reflections. Then the crystal was recentered more accurately using 16 large-angle reflections with 2θ values ranging from 15 to 30°. An ω scan data set was collected with a scan rate of 8°/min, where three check reflections were periodically recorded to monitor the stability and orientation of the crystal. The weak reflections with $I < 5.0\sigma(I)$ were rescanned (maximum of two rescans), and the counts were accumulated to assure good counting statistics. Details of crystal data and other relevant information are summarized in Table I. The intensity measurements were corrected for Lorentz and polarization effects, and an empirical absorption correction was applied on the basis of azimuthal scans of three reflections, which resulted in transmission factors ranging

(11) (a) Tatsumi, K.; Inoue, Y.; Nakamura, A.; Cramer, R. E.; VanDoorne, W.; Gilje, J. W. *Angew. Chem., Int. Ed. Engl.* **1990**, *29*, 422–424. (b) Banister, A. J.; Barr, D.; Brooker, A. T.; Clegg, W.; Cunnington, M. J.; Doyle, M. J.; Drake, S. R.; Gill, W. R.; Manning, K.; Raithby, P. R.; Snaith, R.; Wade, K.; Wright, D. S. *J. Chem. Soc., Chem. Commun.* **1990**, 105–107.

Table I. Crystal Data for $Li_2(thf)_3[Cp^*Ta(S_2)_2]_2(\mu\text{-}O)\cdot THF$ (4), $[Li_2(thf)_2Cp^*TaS_3]_2$ (5a), and $[Li_3(tmeda)_2Cp^*TaS_3Cl]_2(\mu\text{-}tmeda)$ (8)

	4	5a	8
formula	$Li_2Ta_2S_8C_{32}O_4H_{54}\cdot C_4OH_8$	$Li_4Ta_2S_6C_{36}O_4H_{62}$	$Li_6Ta_2S_6Cl_2C_{50}N_{10}H_{110}$
fw	1207.2	1140.9	1518.2
cryst syst	monoclinic	monoclinic	triclinic
space group	$P2_1/n$	$C2/c$	$P\bar{1}$
a, Å	17.81 (2)	24.879 (5)	10.902 (4)
b, Å	13.000 (9)	11.501 (2)	11.169 (3)
c, Å	19.96 (2)	16.669 (3)	17.154 (5)
α, deg	90.0	90.0	83.06 (2)
β, deg	95.91 (7)	99.21 (1)	88.43 (3)
γ, deg	90.0	90.0	64.00 (2)
vol, Å^3	4593 (6)	4709 (1)	1863 (1)
Z	4	4	1
ρ_{calcd}, g/cm^3	1.74	1.61	1.35
μ, cm^{-1}	53.6	48.5	31.7
unique data	5817 ($I > 3.0\sigma(I)$)	4775 ($I > 3.0\sigma(I)$)	8007 ($I > 1.0\sigma(I)$)
data-to-parameter ratio	14.5:1	21.2:1	24.7:1
$R(R_w)$	0.0497 (0.0537)	0.0432 (0.0432)	0.0403 (0.0388)

from 0.5 to 1.00. Examination of systematic absence uniquely determines the space group as $P2_1/n$ (a nonstandard setting of $P2_1/c$, No. 14). Of 7577 unique reflections measured, 5817 observed reflections with $I > 3.0\sigma(I)$ were used for the refinement.

The positions of the two tantalum atoms were determined by direct methods and were confirmed by the Patterson map generated by a SHELX-76 program.[12] The remaining heavy atoms were located in succeeding difference Fourier syntheses and block-diagonal least-squares refinements. Atomic scattering factors for S, O, C, and H were supplied by SHELX-76, and those for Ta and Li were taken from the literature.[13] Four well-behaved THF molecules were located in the asymmetric unit, three of which are bound to Li atoms. Occupancy refinement of the fourth, uncoordinated, THF molecule showed each atom of the crystal solvate to be fully occupied. Anisotropic refinements were applied to non-hydrogen atoms except those of the fourth THF molecule and carbons in the other Li-bound THFs. Hydrogens were located at calculated positions assuming the C–H distance of 0.97 Å, and their isotropic thermal parameters were fixed, while hydrogens of the fourth THF were excluded. The methylene protons were constrained to ride on the carbons to which they are bonded and the methyl groups were treated as rigid groups.

Refinement coverged at $R = 0.0497$ and $R_w = 0.0537$, and the final difference Fourier map showed the maximum residual peak of 1.00 e/Å^3 in the vicinity of the Ta atoms. The atomic positional parameters of all non-hydrogen atoms are listed in Table II along with the equivalent isotropic thermal parameters U_{eq}.

X-ray Crystallographic Study of 5a. A single crystal (0.7 × 0.5 × 0.3 mm) of **5a** was sealed in a thin-walled glass capillary under argon, and intensity data were measured on a Nicolet R3 diffractometer with graphite-monochromated Mo Kα radiation. According to the systematic absences, two monoclinic space groups, Cc (No. 9) and $C2/c$, were possible. Simple E statistics favored the latter centrosymmetric space group, and successful refinement of the structure based on the $C2/c$ group proved the choice to be correct. Data collection was performed using a $\theta/2\theta$ scan technique with a scan rate of 3.0–29.3°/min. Of 5782 reflections, 4775 reflections with $I > 3.0\ \sigma(I)$ were regarded as observed. The data were corrected for Lorentz and polarization effects, and an empirical absorption correction was made using five azimuthal scans (transmission coefficients, 0.94–1.00). Details concerning crystal characteristics and X-ray diffraction methodology are shown in Table I.

The structures was solved by direct methods using a Nicolet SHELXTL PLUS package and was refined straightforwardly by subsequent full-matrix least squares. Atomic scattering factors for S, O, C, and H were supplied by the package and those for Ta and Li were the literature values.[12] There was no crystal solvent, and the Li-bound THF molecules behaved well. Hydrogen atoms were not located and other atoms except for Li's were treated anisotropically. Refinement converged at $R = 0.043$ and $R_w = 0.047$. The final difference Fourier map showed maximum peaks of 0.42 e/Å^3 as ripples near the Ta atoms. The atomic positional parameters and the U_{eq} values are given in Table II. Complete listings of thermal parameters and a table of observed and calculated structure factors are available as supplementary material in ref 6.

X-ray Crystallographic Study of 8. A single crystal of **8** (0.4 × 0.4 × 0.3 mm) was sealed in a thin-walled glass capillary under argon and intensity data were recorded on a Nicolet R3 diffractometer using graphite-monochromated Mo Kα radiation. Least squares analysis of 15 initially measured centering reflections, with 2θ values ranging from 4.9 to 18.7°, determined the cell to be triclinic. The structure was successfully solved and was refined in the centrosymmetric space group $P\bar{1}$. Because of the good diffraction quality of the crystal, 8007 reflections with $I > 1.0\sigma(I)$ were regarded as observed out of 8600 independent reflections measured. The intensity measurements were corrected for Lorentz and polarization effects and for absorption on the basis of six azimuthal scans ranging in 2θ from 7 to 35° (transmission coefficients, 0.55–0.93). The crystal data are summarized in Table I.

The structure was solved with a Nicolet SHELXTL PLUS package, where a Patterson map revealed the Ta position unequivocally. Remaining heavy atoms were located in the succeeding Fourier maps. The inner ring carbons of Cp* were treated as a rigid group. The difference Fourier maps revealed the presence of two Li-bound complete tmeda ligands and another with the ethylene backbone lying on the crystallographically imposed inversion center. As anisotropic refinement was applied to all heavy-atoms except for the lithiums, the ethylene carbons of the latter tmeda, C(1), were found to be disordered with the occupancy factors of 0.80 (2) and 0.20 (2). We label the major and minor carbon positions as C(1a) and C(1b), respectively. All hydrogen atoms were included in the final refinement at the calculated positions, as constrained to ride on the carbons, where the isotropic thermal parameters were fixed and the C–H bond lengths were idealized at 0.97 Å. The resulting R values are $R = 0.0403$ and $R_w = 0.0388$. The maximum remaining peak was 0.55 e/Å^3. The greatest shift in the final cycle belongs to the disordered C(1), which is 12% of its estimated standard shift. The atomic positional parameters and the U_{eq} values are given in Table II.

Molecular Orbital Calculations. Molecular orbital calculations of the extended Hückel type, using the modified Wolfsberg–Helmholz formula were carried out.[14] The parameters for Ta were taken from the previous work,[15] while those of S, C, and H are the standard ones. Due to the highly positive nature of Li in the molecules studied here, we modified its orbital

(12) Sheldrick, G. M.; SHLEX-76: Program for Crystal Structure Determination. University of Cambridge, England, 1976.
(13) *Internatinal Tables for X-Ray Crystallography*; Kynoch: Birmingham, England, 1974; Vol. IV.

Table II. Fractional Atomic Coordinates and Equivalent Isotropic Thermal Parameters of Non-Hydrogen Atoms in 4, 5a, and 8 with Esd's in Parentheses

atom	*x*	*y*	*z*	U_{eq}, Å^2	atom	*x*	*y*	*z*	U_{eq}, Å^2
			(a) $Li_2(thf)_3[Cp^*Ta(S_2)_2]_2(\mu\text{-}O)\cdot THF$ (**4**)						
Ta(1)	0.19871 (2)	0.20170 (3)	0.01316 (2)	0.034	C(15)	0.1072 (6)	0.5093 (9)	−0.1358 (6)	0.051
Ta(2)	0.21556 (2)	0.42240 (3)	−0.06748 (2)	0.035	C(16)	0.1613 (8)	0.686 (1)	−0.0943 (8)	0.072
S(1)	0.2039 (2)	0.2601 (2)	0.1349 (1)	0.051	C(17)	0.2920 (8)	0.612 (1)	−0.1773 (7)	0.076
S(2)	0.2929 (2)	0.1693 (3)	0.1101 (2)	0.057	C(18)	0.2503 (9)	0.394 (1)	−0.2388 (7)	0.075
S(3)	0.3020 (2)	0.1532 (2)	−0.0558 (2)	0.054	C(19)	0.0829 (8)	0.342 (1)	−0.2036 (7)	0.070
S(4)	0.2178 (2)	0.2330 (2)	−0.1119 (1)	0.045	C(20)	0.0290 (7)	0.528 (1)	−0.1158 (8)	0.078
S(5)	0.0993 (1)	0.3457 (2)	−0.0183 (1)	0.041	O(2)	0.2511 (5)	0.5410 (8)	0.1591 (6)	0.081
S(6)	0.1390 (2)	0.4827 (2)	0.0220 (2)	0.047	C(21)	0.1883 (9)	0.538 (1)	0.1988 (9)	0.089
S(7)	0.3122 (2)	0.5420 (3)	−0.0169 (2)	0.058	C(22)	0.152 (1)	0.636 (2)	0.189 (1)	0.115
S(8)	0.3564 (2)	0.4294 (3)	−0.0741 (2)	0.063	C(23)	0.204 (1)	0.704 (2)	0.162 (1)	0.159
O(1)	0.2553 (3)	0.3356 (5)	0.0112 (3)	0.037	C(24)	0.270 (1)	0.643 (2)	0.151 (1)	0.147
Li(1)	0.265 (1)	0.427 (2)	0.089 (1)	0.059	O(3)	0.4657 (4)	0.2425 (8)	0.0380 (5)	0.075
Li(2)	0.362 (1)	0.302 (2)	0.026 (1)	0.064	C(31)	0.521 (1)	0.275 (2)	0.002 (1)	0.108
C(1)	0.0832 (6)	0.1120 (8)	0.0415 (5)	0.041	C(32)	0.582 (1)	0.199 (2)	0.012 (1)	0.108
C(2)	0.0826 (6)	0.1082 (8)	−0.0297 (5)	0.044	C(33)	0.567 (1)	0.134 (2)	0.066 (1)	0.143
C(3)	0.1410 (7)	0.0421 (9)	−0.0441 (6)	0.052	C(34)	0.483 (1)	0.150 (2)	0.072 (1)	0.117
C(4)	0.1789 (6)	0.0077 (8)	0.0158 (6)	0.050	O(4)	0.3835 (4)	0.4066 (7)	0.1239 (4)	0.057
C(5)	0.1425 (6)	0.0483 (8)	0.0694 (6)	0.047	C(41)	0.4415 (8)	0.481 (1)	0.1157 (7)	0.071
C(6)	0.0242 (7)	0.163 (1)	0.0782 (7)	0.072	C(42)	0.492 (1)	0.476 (2)	0.178 (1)	0.142
C(7)	0.0188 (7)	0.146 (1)	−0.0778 (7)	0.078	C(43)	0.470 (1)	0.392 (2)	0.220 (1)	0.123
C(8)	0.1538 (9)	0.003 (1)	−0.1141 (7)	0.089	C(44)	0.3959 (9)	0.368 (1)	0.1906 (8)	0.086
C(9)	0.2431 (8)	−0.068 (1)	0.025 (1)	0.093	O(5)	0.466 (2)	0.093 (2)	0.824 (1)	0.250
C(10)	0.1559 (8)	0.018 (1)	0.1413 (7)	0.079	C(51)	0.433 (2)	0.196 (3)	0.794 (2)	0.191
C(11)	0.1664 (6)	0.5842 (8)	−0.1270 (6)	0.049	C(52)	0.498 (3)	0.242 (3)	0.776 (2)	0.230
C(12)	0.2253 (6)	0.5491 (9)	0.1639 (6)	0.050	C(53)	0.561 (2)	0.191 (3)	0.796 (2)	0.181
C(13)	0.2051 (7)	0.4513 (9)	−0.1914 (6)	0.052	C(54)	0.546 (2)	0.084 (2)	0.816 (2)	0.182
C(14)	0.1320 (6)	0.4277 (8)	−0.1750 (5)	0.044					
			(b) $[Li_2(thf)_2Cp^*TaS_3]_2$ (**5a**)						
Ta	0.1445 (1)	0.3173 (1)	0.0029 (1)	0.029	C(10)	0.0761 (8)	0.512 (3)	−0.136 (2)	0.203
S(1)	0.2069 (1)	0.4396 (2)	0.0723 (2)	0.040	O(1)	0.1594 (3)	−0.0291 (8)	−0.1165 (5)	0.063
S(2)	0.1708 (1)	0.2827 (3)	−0.1191 (1)	0.047	C(11)	0.1593 (6)	−0.025 (1)	−0.2040 (8)	0.081
S(3)	0.1605 (1)	0.1444 (2)	0.0718 (1)	0.040	C(12)	0.1015 (7)	−0.014 (2)	−0.2390 (9)	0.101
C(1)	0.0495 (5)	0.332 (2)	−0.0693 (7)	0.081	C(13)	0.0726 (7)	−0.089 (2)	−0.182 (1)	0.115
C(2)	0.0470 (4)	0.290 (1)	0.0096 (9)	0.063	C(14)	0.1092 (6)	−0.082 (1)	−0.1015 (9)	0.080
C(3)	0.0651 (5)	0.374 (2)	0.0645 (7)	0.084	O(2)	0.2449 (3)	0.2867 (8)	0.2602 (4)	0.061
C(4)	0.0784 (4)	0.471 (1)	0.021 (1)	0.089	C(21)	0.2870 (6)	0.239 (1)	0.3194 (6)	0.068
C(5)	0.0710 (5)	0.445 (2)	−0.061 (1)	0.084	C(22)	0.2843 (8)	0.302 (2)	0.3974 (8)	0.102
C(6)	0.0300 (7)	0.269 (3)	−0.151 (1)	0.210	C(23)	0.2342 (8)	0.371 (2)	0.384 (1)	0.118
C(7)	0.0228 (6)	0.169 (2)	0.028 (2)	0.181	C(24)	0.2131 (6)	0.374 (2)	0.2957 (8)	0.089
C(8)	0.0693 (8)	0.369 (4)	0.157 (1)	0.245	Li(1)	0.1995 (7)	0.092 (1)	−0.048 (1)	0.041
C(9)	0.0951 (7)	0.588 (2)	0.060 (3)	0.283	Li(2)	0.2356 (7)	0.255 (2)	0.147 (1)	0.045
			(c) $Li_3(tmeda)_2[Cp^*TaS_3Cl]_2(\mu\text{-}tmeda)$ (**8**)						
Ta	0.1001 (1)	0.2382 (1)	0.3174 (1)	0.035	C(1b)	−0.0301	0.4709	0.9674	0.044
S(1)	0.2937 (1)	0.1778 (1)	0.2446 (1)	0.043	C(2)	0.2984 (7)	0.3311 (8)	1.0323 (4)	0.092
S(2)	0.0621 (1)	0.0506 (1)	0.3264 (1)	0.047	C(3)	0.1746 (9)	0.5134 (8)	1.1048 (5)	0.095
S(3)	−0.0646 (1)	0.3952 (1)	0.2337 (1)	0.051	N(20)	0.8689 (5)	−0.0403 (5)	0.1915 (3)	0.062
Cl	0.0385 (2)	0.1407 (2)	0.0868 (1)	0.078	N(21)	0.7009 (5)	0.2485 (5)	0.1983 (4)	0.076
C(10)	0.2365	0.2556	0.4251	0.056	C(20)	−0.3549 (8)	0.1568 (8)	0.1799 (6)	0.113
C(11)[a]	0.1581 (4)	0.1916 (3)	0.4606 (2)	0.056	C(21)	−0.272 (1)	0.0177 (9)	0.2157 (7)	0.122
C(12)	0.0181	0.2846	0.4515	0.056	C(22)	−0.057 (1)	−0.1614 (8)	0.2457 (6)	0.134
C(13)	0.0100	0.4062	0.4104	0.056	C(23)	−0.120 (1)	−0.0736 (9)	0.1117 (4)	0.111
C(14)	0.1450	0.3883	0.3940	0.053	C(24)	−0.3394 (9)	0.290 (1)	0.2770 (6)	0.120
C(15)	0.3901 (7)	0.1976 (8)	0.4279 (4)	0.086	C(25)	−0.3446 (9)	0.3643 (8)	0.1393 (6)	0.119
C(16)	0.2125 (9)	0.0529 (6)	0.5079 (3)	0.090	N(30)	0.6187 (6)	0.1401 (5)	0.8572 (3)	0.070
C(17)	−0.0993 (9)	0.2586 (9)	0.4832 (4)	0.098	N(31)	0.5774 (6)	0.2087 (5)	0.6882 (3)	0.072
C(18)	−0.1160 (8)	0.5373 (7)	0.3963 (4)	0.091	C(30)	0.5135 (8)	−0.2398 (8)	1.1804 (4)	0.103
C(19)	0.188 (1)	0.4888 (8)	0.3529 (4)	0.096	C(31)	0.5023 (9)	−0.3023 (8)	1.2571 (5)	0.103
Li(1)	0.268 (1)	−0.031 (1)	0.2401 (6)	0.067	C(32)	0.307 (1)	−0.2011 (9)	1.1064 (7)	0.127
Li(2)	0.1094 (8)	0.2869 (8)	0.1391 (5)	0.048	C(33)	0.4086 (9)	−0.0523 (8)	1.0819 (4)	0.096
Li(3)	−0.080 (1)	−0.031 (1)	0.2401 (6)	0.054	C(34)	0.507 (1)	−0.1623 (8)	1.3517 (5)	0.106
N(1)	0.1629 (4)	0.4148 (4)	1.0620 (2)	0.053	C(35)	0.368 (1)	−0.2757 (9)	1.3732 (6)	0.169
C(1a)[b]	0.0724 (7)	0.4682 (7)	0.9906 (4)	0.058					

[a] Used as the pivot atom when the five-membered ring of Cp* was fixed. [b] Occupancy factors are C(1) = 0.80 (2) and C(1a) = 0.20 (2).

exponent from the standard value of 0.65 to 1.00. These parameters are listed in Table III.

Tantalum to sulfur distances were fixed at 2.28 Å. For the Li-containing model complexes, Li_2CpTaS_3 and Li_3TaS_4, a coplanar LiS_2Ta unit was assumed with a Li–S distance of 2.50 Å. Other geometrical parameters include C–C = 1.40 Å, C–H = 1.09 Å, and Cp(centroid)–Ta = 2.16 Å, for $CpTaS_3^{2-}$ and Li_2CpTaS_3, and Ta–H(cis) = 1.8 Å and Ta–H(trans) = 1.9 Å, for octahedral $TaS(H)_5$.

(14) (a) Summerville, R.; Hoffmann, R. *J. Am. Chem. Soc.* **1976**, *98*, 7240–7254. (b) Ammeter, J. H.; Bürgi, H.-B.; Thibeault, J. C.; Hoffmann, R. *J. Am. Chem. Soc.* **1978**, *100*, 3686–3692.

(15) Tatsumi, K.; Matsubara, I.; Inoue, Y.; Nakamura, A.; Miki, K.; Kasai, N. *J. Am. Chem. Soc.* **1989**, *111*, 7766–7777.

Results and Discussion

Synthesis and Characterization. $Li_2(thf)_3[Cp^*Ta(S_2)(\mu\text{-}S_2)]_2(\mu\text{-}O)\cdot THF$ (4). The preparation of sulfide

Table III. Atomic Parameters Used for Extended Hückel Calculations

atom	orbital	H_{ii}, eV	exponent[a]
Ta	6s	−9.36	2.280
	6p	−6.23	2.241
	5d	−11.04	4.762 (0.6700) + 1.938 (0.5592)
S	3s	−20.0	1.817
	3p	−13.3	1.817
C	2s	−21.4	1.625
	2p	−11.4	1.625
Li	2s	−5.4	1.000
	2p	−3.5	1.000
H	1s	−13.6	1.3

[a] The numbers in parentheses are contraction coefficients used in the double-ζ expansion.

complexes of early transition metals is often beset with problems arising from the propensity of sulfide and polysulfide anions to form insoluble polymeric residues.[16] In the hope that the presence of Cp* and a rigid Ta–O–Ta skeleton might avoid the problem, we first examined the reaction of $(Cp^*TaCl_3)_2(\mu\text{-}O)$ with 4 equiv of Li_2S_2 in a THF solution. Indeed, evaporation of the solvent and

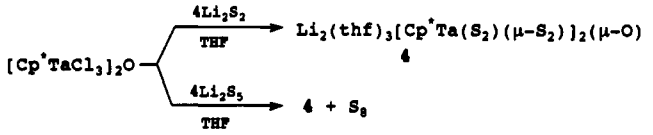

extraction of the crude product in benzene followed by recrystallization from THF afforded yellow crystals of $Li_2(thf)_3[Cp^*Ta(S_2)(\mu\text{-}S_2)]_2(\mu\text{-}O)\cdot THF$ (**4**). The yield of isolated crystals was ca. 40%, so that the total yield should be higher. Complex **4** is relatively stable in the air, but 1 equiv of THF is rapidly lost either under vacuum or in argon, which is consistent with the presence of the crystal solvent in the X-ray-derived structure. Thus the elemental analysis and the ^1H NMR data fit the formula $Li_2(thf)_3[Cp^*Ta(S_2)(\mu\text{-}S_2)]_2(\mu\text{-}O)$. According to the room-temperature ^1H NMR spectrum in C_6D_6, the two Cp* ligands are equivalent in solution, the singlet signal of which appears at 2.10 ppm, and so are the three THF molecules. The UV–visible spectrum in THF is featureless in the 300–800-nm range.

The use of Li_2S_5 (4 equiv), instead of Li_2S_2, also resulted in formation of **4**, suggesting that the Cp*Ta–O–TaCp* unit accomodates sulfur specifically in the disulfide(2−) form. In this case, however, **4** and S_8 cocrystallize and their manual separation is required.

$[Li_2(thf)_2Cp^*MS_3]_2$ (M = Ta, (5a), Nb (5b)). We then carried out the reaction between Cp^*TaCl_4 and Li_2S_2 (2 equiv) in THF, only to find that an uncharacterizable

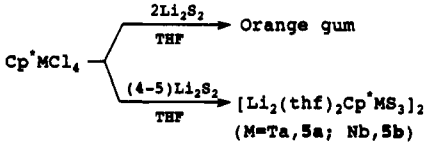

orange-colored gum was formed after a workup similar to that used to isolate **4**. However, when the amount of Li_2S_2 was increased to 4–5 equiv, we were able to isolate $[Li_2(thf)_2Cp^*TaS_3]_2$ (**5a**) as light yellow crystals in ca. 30% yield.[17] With this stoichiometry established, it is obvious that at least 3–4 equiv of Li_2S_2 is necessary for the formation of **5a**. Although the fate of the excess sulfur could not be traced, a Cp^*TaCl_4/Li_2S_2 1:3 molar ratio would lead to **5a** + 4LiCl + $^3/_8S_8$, while a 1:4 molar ratio would give rise to **5a** + 4LiCl + Li_2S_5. The ^1H NMR spectrum of **5a** in THF-d_8 shows a singlet at 2.03 ppm for Cp* protons along with a set of THF signals. The UV–visible spectrum is characterized by an absorption at 302 nm.

The analogous Nb complex, $[Li_2(thf)_2Cp^*NbS_3]_2$ (**5b**), was prepared in the Cp^*NbCl_4/Li_2S_2 (1:4–5) reaction system as yellow crystals in 5% yield. Its Raman spectrum is nearly identical to that of the Ta complex **5a**. Also the upfield shift of the ^1H NMR signal arising from Cp* of **5b** (2.00 ppm), relative to **5a**, is very slight. On the other hand, we noticed in the electronic spectrum that the absorption at 302 nm characteristic of **5a** shifts significantly to a longer wavelength (341 nm) for the Nb complex, **5b**. Because of their high intensities and a d^0 electronic configuration of the metal, the observed absorption is probably due to a sulfur-to-metal charge-transfer transition. Interestingly, the Ta to Nb red (bathochromic) shift of 0.47 eV is comparable to those found for the low-energy absorption bands of $(A)[M(SCH_2CH_2S)_3]$ (A = Ph_4P, Et_4N; M = Ta, Nb), $(A)[M(SCH_2CH_2CH_2S)_3]$, and $(A)[M(ndt)_3]$, where the Ta to Nb red shifts are 0.41–0.52 eV for the ethanedithiolate complexes, 0.46–0.48 eV for the propanedithiolate complexes,[18a] and 0.35–0.45 eV for the norbornane-*exo*-2,3-dithiolate complexes.[15]

$[Li_2(dme)Cp^*TaS_3]_2$ (6) and $Li_2(tmeda)_2Cp^*TaS_3$ (7). In THF molecules coordinated at Li in **5a** can be readily replaced by DME and TMEDA. Thus treatment of **5a** in DME, and subsequent addition of hexane produced light yellow needles formulated as $Li_2(dme)Cp^*TaS_3$ (**6**) on the basis of integration of the ^1H NMR spectrum. The yield is nearly quantitative. On the other hand, a toluene suspension of **5a** became a homogeneous yellow solution upon addition of excess TMEDA, from which light yellow microcrystals of $Li_2(tmeda)_2Cp^*TaS_3$ (**7**) were obtained, again in a quantitative yield.

We have not succeeded in obtaining crystals of **6** and **7** suitable for X-ray diffraction work, and therefore structural deductions must be based on less direct considerations. Their Raman signals arising from Ta=S stretching vibrations are very similar to those of **5a**, and so are the UV spectra (305 nm for **6** and 304 nm for **7**). The Cp* resonances in the ^1H NMR spectra appear as a sharp singlet at 2.08 ppm for **6** and at 2.45 ppm for **7**. From these data, it is reasonable to expect that a piano-stool geometry of the $Cp^*TaS_3^{2-}$ fragment remains intact upon replacement of THF in **5a** by DME or TMEDA, and that Li atoms are probably bound to sulfurs.

Coordination of TMEDA to Li cations is manifest by the ^1H NMR spectrum for **7**. The methyl proton signal is shifted to a lower field (2.42 ppm) relative to its methylene signal (2.14 ppm), while those of free tmeda come at 2.14 ppm (CH_3) and 2.36 ppm (CH_2). This reversal of the methyl vs methylene proton chemical shifts has also been found in the spectrum of the Li-bound TMEDA in $Li_2(tmeda)_2S_6$.[11] In the case of **6**, the DME methyl and methylene proton signals appear as sharp singlets (3.26 ppm (CH_3) and 3.43 ppm (CH_2)), the chemical shifts of

(16) See for example ref 25 and: Schunn, R. A.; Firtchie, C. J., Jr.; Prewitt, C. T. *Inorg. Chem.* **1966**, *5*, 892–899.

(17) The yellowish white solid obtained from the mother liquid also contains **5a**, according to ^1H NMR, and the combined yield is around 50–60%.

(18) (a) Tatsumi, K.; Matsubara, I.; Sekiguchi, Y.; Nakamura, A.; Mealli, C. *Inorg. Chem.* **1989**, *28*, 773–780. (b) Tatsumi, K.; Kawaguchi, H.; Tani, K. *Angew. Chem., Int. Ed. Engl.*, in press.

Scheme II

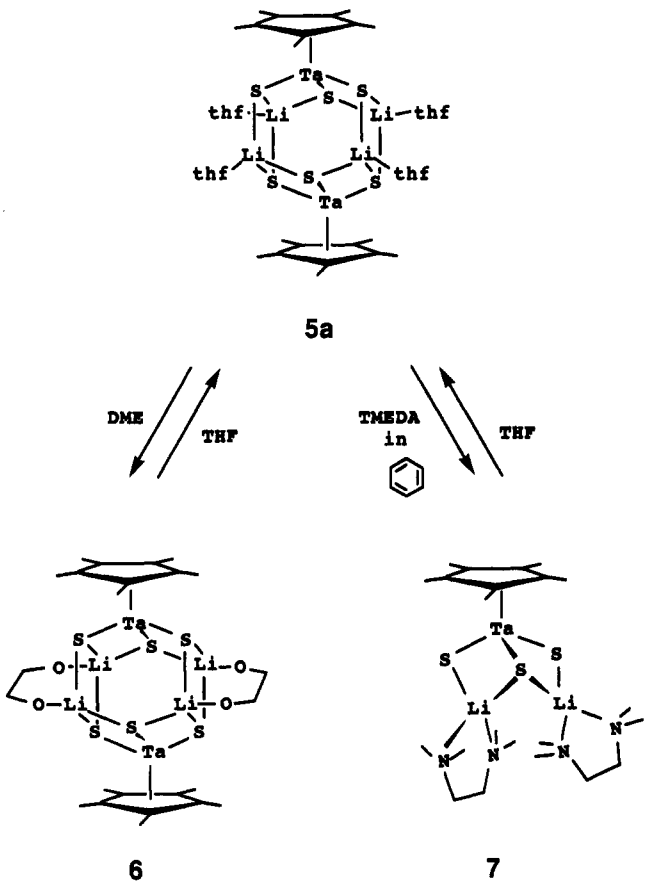

which remain close to those of the singlet signals for free DME (3.25 ppm (CH_3) and 3.41 ppm (CH_2)).

An obvious difference between **6** and **7** is the number of the chelate "ligands". Provided that each Li possesses a tetrahedral coordination sphere, the 2:1 Li:DME ratio for **6** is indicative of a dimeric structure as shown in Scheme II (left), presumably with a hexagonal prismatic $Ta_2S_6Li_4$ core. On the other hand, having the 1:1 Li:TMEDA ratio, the most rational structure of **7** would be a monomeric one (Scheme II right). In fact, the selenido analog, $Li_2(tmeda)_2Cp^*TaSe_3$, was found to have a monomeric structure similar to **7**.[18b] The higher solubility of **7** in benzene relative to **5a** and **6** is consistent with the monomeric structure of **7**. Also the downfield shift of the Cp* proton chemical shifts in going from **6** (2.08 ppm) to **7** (2.45 ppm) may be due to their structural difference. Unfortunately, molecular weight measurements in terms of cryoscopy in benzene have been hampered due to relative low solubility.

Addition of THF to **6** or **7** in THF regenerated **5a** in nearly quantitative yields. Thus the Li-bound ligands are labile and are likely to participate in a dynamic equilibrium involving a partially desolvated $Cp^*TaS_3Li_2$ complex and free ligands. On the other hand, we have not been successful in replacing the Li cations of either **5a**, **5b**, **6**, and **7** (and **8**) by organic cations such as PPh_4^+ or NR_4^+ (R = Me, Et).[19] The Li cations appear to be bound strongly to sulfurs.

$[Li_3(tmeda)_2Cp^*TaS_3Cl]_2(\mu$-tmeda) (8). Our attempt to synthesize **7** directly from the reaction system Cp^*TaCl_4 + (4–5)Li_2S_2 + TMEDA failed. Instead, when the oily

(19) The relatively instable nature of these complexes in acetonitrile solution also makes the cation-exchange reactions difficult.

Scheme III

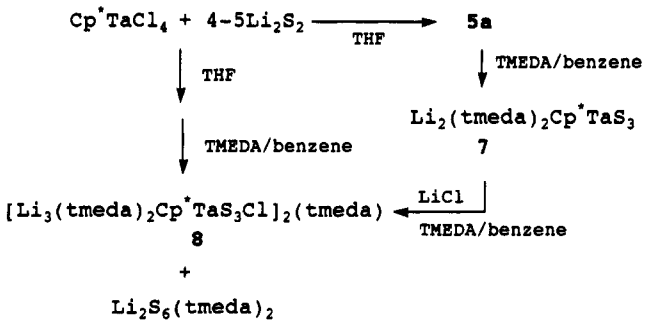

residue obtained from the reaction between Cp^*TaCl_4 and Li_2S_2 was extracted with TMEDA/benzene, light yellow crystals formulated as $[Li_3(tmeda)_2Cp^*TaS_3Cl]_2(\mu$-tmeda) (**8**) were obtained upon recrystallization from THF/hexane. Thus, under these particular conditions the preformed $Cp^*TaS_3Li_2$ fragment takes up LiCl from the reaction mixture and generates an intriguing $Cp^*TaS_3Li_3Cl$ cluster. Treatment of **7** with LiCl and TMEDA in benzene also afforded complex **8**. These reaction patterns are depicted in Scheme III.

It is not obvious why the presence of TMEDA promotes incorporation of LiCl into the TaS_3Li_2 core. However, once the Li_3TaS_3Cl core with Li-bound TMEDA ligands is formed, the skeletal structure seems to be stable in THF. Complex **8** can be repeatedly recrystallized from THF, during which time LiCl does not come off.

The UV–visible spectrum of **8** exhibits an absorption at 301 nm, which is characteristic of the "$Cp^*TaS_3Li_2$" type clusters. The ^1H NMR spectrum in C_6D_6 is interesting. At room temperature, there appear resonances for only one type of TMEDA group (2.24 ppm (CH_2), 2.30 ppm (CH_3)) along with a peak associated with Cp*(2.43 ppm), where the reversal of the TMEDA methyl and methylene proton chemical shifts was again noticed, implying interactions between Li and TMEDA. Furthermore, as TMEDA is added to a solution of **8**, the above TMEDA-based resonances moved asymptotically toward those for free TMEDA, while the peak for Cp* remains unshifted. The appearance of only one set of TMEDA signals indicates that the molecule is fluxional in solution and that not only the two chelating η^2-TMEDA molecules but also the bridging μ-TMEDA is involved in the exchange processes. This fluxional behavior will be discussed later in this paper. Note that the Cp* proton chemical shift resembles that of **7** and differs from those of **5a** and **6**.

$Li_2(thf)_2Cp^*_3Ta_3S_6$ (9). The reaction of Cp^*TaCl_4 with 4–5 equiv of Li_2S followed by workup similar to that for the analogous reaction with Li_2S_2 yielded dark red crystals

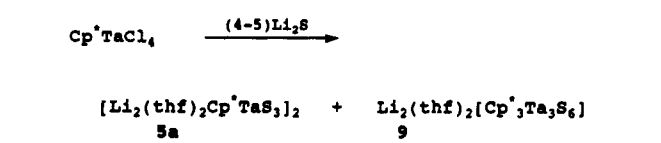

in addition to a smaller amount of light yellow crystals of **5a**. A preliminary X-ray structure determination showed that the red complex **9** comprises a Ta_3 triangle and six monosulfides bridging Ta atoms above and below the edges. At each corner of the Ta_3 triangle, a Cp* ring caps tantalum to give a $Cp^*_3Ta_3S_6^{2-}$ structure, and then two lithium cations triply bridge sulfurs at the triangle faces defined by the trigonal prismatic S_6 skeleton. Each lithium

is further bonded by a THF molecule, completing the tetrahedral coordination geometry (see F). The diamag-

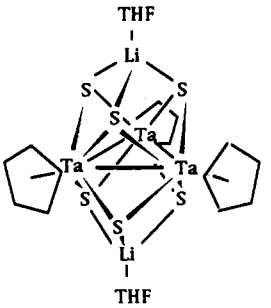

F

netic complex **9** is soluble in both THF and toluene, showing a characteristic absorption at 510 nm in its UV–visible spectrum.

A detailed account of the structure and physicochemical properties of **9** will be described elsewhere.[20] We only comment here that the formal oxidation states of the Ta atoms are 2Ta(IV) + Ta(V), based on its formula, and therefore a partial reduction of tantalum takes place during the reaction with Li_2S. The $Cp^*_3Ta_3S_6^{2-}$ cluster geometry has a resemblance to $Cp^*_3Re_3O_6^{2+}$,[21] although the latter oxide cluster carries two more d electrons than the sulfide cluster. Interestingly, the presence of even a slight excess of sulfur in Li_2S inhibits the reduction and gives rise only to **5a**. On the other hand, use of "Li_3S" instead of Li_2S or addition of Li metal in the Cp^*TaCl_4/(4–5)Li_2S reaction system does not promote or even deters formation of **9**, which rules out a mechanism based on Li-promoted reduction. We believe that Li_2S itself plays a major role in the partial reduction of tantalum.

Solid-State Structure of $Li_2(thf)_3[Cp^*Ta(S_2)(\mu\text{-}S_2)]_2(\mu\text{-}O)\cdot THF$ (4). The monoclinic unit cell of **4** contains four crystallographically related, discrete binuclear Ta complexes as well as four THF solvent molecules which pack with no abnormally short intermolecular contacts. Figure 1 presents structures of the entire molecule and of its $[Cp^*Ta(S_2)(\mu\text{-}S_2)]_2(\mu\text{-}O)$ portion, where the numbering scheme is adopted. Selected bond distances and angles are listed in Table IV.

The molecule contains a bent Cp*Ta–O–TaCp* spine with the Ta–O–Ta angle of 11.4 (3)°. Then two disulfide-(2–) ligands coordinate at each Ta atom, and one of them provides a semibridging sulfur atom (S(4) or S(5)) which is also bound to the other Ta. This type of η^2,η^1-disulfide group has been found, e.g., in the structures of $[Mo_2Fe_6S_{12}(S\text{-}p\text{-}C_6H_4Br)_6]^{4-}$,[22] $Cp_2Cr_2(CO)_5S_2$,[23] $[Mo_4(NO)_4S_{13}]^{4-}$,[24] and $Cp^*_2Mo_2S_{10}$.[25] And the geometry of the entire $[Ta(S_2)]_2(\eta^2,\eta^1\text{-}S_2)_2(\mu\text{-}O)^{2-}$ unit resembles closely that of $[Mo(S_2)]_2(\eta^2,\eta^1\text{-}S_2)_2(\mu\text{-}S)$ in $[\{OMo(S_2)_2\}_2S]^{2-}$.[26]

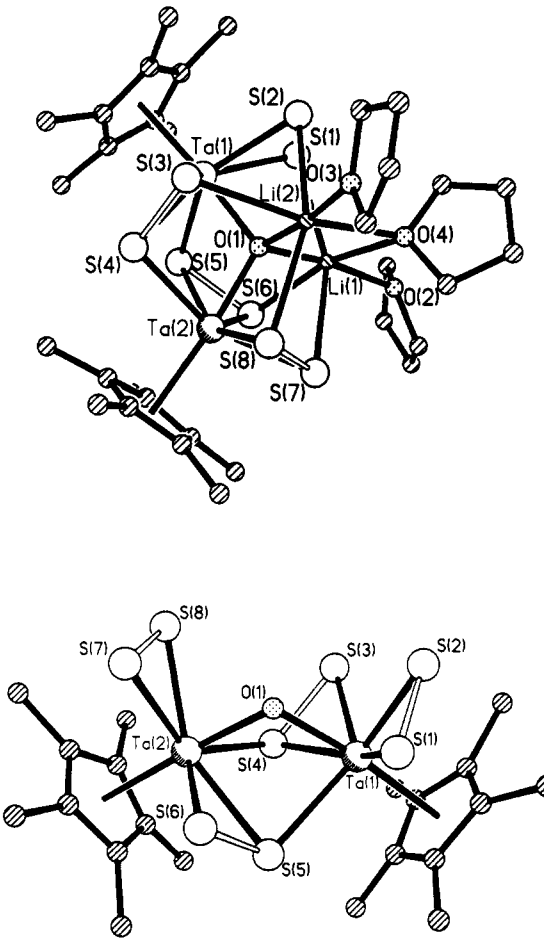

Figure 1. Molecular structure and atom-labeling scheme for $Li_2(thf)_3[Cp^*Ta(S_2)_2]_2(\mu\text{-}O)\cdot THF$ (**4**): (top) the entire molecule where the uncoordinate solvent molecule is excluded; (bottom) side view of the $[Cp^*Ta(S_2)_2]_2(\mu\text{-}O)$ portion.

Table IV. Selected Bond Distances (Å) and Bond Angles (deg) for $Li_2(thf)_3[Cp^*Ta(S_2)_2]_2(\mu\text{-}O)\cdot THF$ (4) with Esd's in Parentheses

Ta(1)–S(1)	2.538 (3)	S(1)–Ta(1)–S(2)	49.0 (1)
Ta(1)–S(2)	2.464 (3)	S(2)–Ta(1)–S(3)	84.7 (1)
Ta(1)–S(3)	2.490 (3)	S(3)–Ta(1)–S(4)	47.8 (1)
Ta(1)–S(4)	2.586 (3)	S(4)–Ta(1)–S(5)	78.9 (1)
Ta(1)–S(5)	2.608 (3)	S(4)–Ta(2)–S(5)	78.8 (1)
Ta(1)–O(1)	2.013 (6)	S(5)–Ta(2)–S(6)	47.7 (1)
Ta(2)–S(4)	2.618 (3)	S(6)–Ta(2)–S(7)	85.3 (1)
Ta(2)–S(5)	2.581 (3)	S(7)–Ta(2)–S(8)	48.8 (1)
Ta(2)–S(6)	2.483 (3)	Ta(1)–O(1)–Ta(2)	111.4 (3)
Ta(2)–S(7)	2.459 (3)	Li(1)–O(1)–Li(2)	91 (1)
Ta(2)–S(8)	2.527 (3)	O(2)–Li(1)–O(4)	92.8 (8)
Ta(2)–O(1)	2.003 (6)	O(3)–Li(2)–O(4)	92.9 (8)
S(1)–S(2)	2.076 (4)	Li(1)–O(4)–Li(2)	74.5 (8)
S(3)–S(4)	2.058 (4)	S(1)–Li(1)–S(7)	150.9 (8)
S(5)–S(6)	2.050 (4)	S(2)–Li(2)–S(8)	151.7 (8)
S(7)–S(8)	2.062 (4)	O(1)–Li(1)–O(2)	165 (1)
Li(1)–O(1)	1.95 (2)	O(1)–Li(2)–O(3)	170 (1)
Li(1)–O(2)	2.07 (2)		
Li(1)–O(4)	2.17 (2)		
Li(1)–S(1)	2.64 (2)		
Li(1)–S(6)	2.60 (2)		
Li(1)–S(7)	2.79 (2)		
Li(2)–O(1)	1.94 (2)		
Li(2)–O(3)	2.00 (2)		
Li(2)–O(4)	2.38 (2)		
Li(2)–S(2)	2.78 (2)		
Li(2)–S(3)	2.68 (2)		
Li(2)–S(8)	2.59 (2)		

The coordination environments of the two Ta sites are practically the same. The geometry about each Ta is best

(20) Tatsumi, K.; Kawaguchi, H.; Inoue, Y.; Nakamura, A.; Cramer, R. E. To be published.

(21) (a) Herrmann, W. A.; Serrano, R.; Ziegler, M. L.; Pfisterer, H.; Nuber, B. *Angew. Chem., Int. Ed. Engl.* **1985**, *24*, 50–51. (b) Herrmann, W. A.; Serrano, R.; Küsthardt, U.; Guggolz, E.; Nuber, B.; Ziegler, M. L. *J. Organomet. Chem.* **1985**, *287*, 329–344. (c) Hofmann, P.; Rösch, N. *J. Chem. Soc., Chem. Commun.* **1986**, 843–844.

(22) Kovacs, J. A.; Bashkin, J. K.; Holm, R. H. *J. Am. Chem. Soc.* **1985**, *107*, 1784–1786.

(23) Goh, L. Y.; Hambley, T. W.; Robertson, G. B. *J. Chem. Soc., Chem. Commun.* **1983**, 1458–1460.

(24) Müller, A.; Eltzner, W.; Mohan, N. *Angew. Chem., Int. Ed. Engl.* **1979**, *18*, 168–169.

(25) Rakowski, DuBois, M.; DuBois, D. L.; VanDerveer, M. C.; Haltiwanger, R. C. *Inorg. Chem.* **1981**, *20*, 3064–3071.

described as a distorted pentagonal bipyramid, with five S atoms occupying the equatorial sites, with the axial sites taken by Cp* and μ-O (i.e., O(1)). As a matter of fact, the "equatorial" S atoms are approximately coplanar (maximum deviation, 0.032 or 0.048 Å), and the nearly linear Cp*(centroid)–Ta–O(1) axial direction bond (173.8 or 174.5°) stands perpendicular to the equatorial S_5 plane. Each S_5 plane is nearly parallel to the corresponding C_5 plane of Cp* (dihedral angle = 3.7 or 2.4°). Each Ta atom is displaced from the S_5 plane toward Cp* by 0.575 or 0.582 Å (Cp*(centroid)–Ta = 2.214 or 2.205 Å), and the Ta–Ta distance is nonbonding at 3.318 (1) Å. The Ta–S vectors are staggered with respect to the C–Me vectors of Cp*. The Ta–S distances range from 2.464 (3) to 2.618 (3) Å, where bonds to the semibridging sulfur are long and the others fall in the normal Ta–S single-bond distances. As for the S–S bonds, both the S–S distances (2.050 (4)–2.076 (4) Å) and the IR band for S–S stretching vibrations (518 cm^{-1}) compare well with those in $[OMo(S_2)_2]_2S^{2-}$.

The two lithiums are not innocent countercations but are bound strongly to the bridging O(1) atom. As a result, O(1) resides in a slightly twisted tetrahedral cavity defined by two Ta and two Li atoms. Departure of the cavity from actual tetrahedral symmetry is reflected by the dihedral angle (78.8°) between the Li_2O and Ta_2O planes that would be 90° under this symmetry. Also the Li–O1–Li angle of 91 (1)° deviates from the ideal angle. Each lithium atom is further coordinated by two oxygens, O(2) (or O(3)) and O(4), from THF molecules, and by three sulfur atoms, thus forming a distorted octahedral coordination geometry. One of these THF molecules is terminally bound while the other bridges between the two lithiums. The Li–O distances are variegated ranging from 1.94 (2) to 2.38 (2) Å; the shortest are those involving the "μ^4"-O(1), and the longest are those of the bridging THF. It is known that Li–O bond lengths vary substantially depending on coordination environments,[27] and the diversity of Li–O distances observed for 4 is not surprising considering the difference in nature of the O donors attached to Li. On the other hand, all the Li–S bonds are rather weak. The observed lengths of 2.59 (2)–2.79 (2) Å are at the long end of known Li–S distances.[11,28] Interestingly, sulfurs, which do not bridge two tantalums, interact with lithium instead, so that all the sulfur atoms link two metals, either Ta–Ta or Ta–Li.

The bent Ta–O(1)–Ta bond contrasts to the linear Ta–O–Ta linkage of related complexes, particularly $[Cp^*Ta(CH_3)_3]_2(\mu$-O). Two obvious differences between 4 and $[Cp^*Ta(CH_3)_3]_2(\mu$-O) are that the former has semibridging sulfurs as well as the oxide between the Ta atoms and that it has Li bound to the oxide. In principle, either factor can stabilize the bent Ta–O–Ta structure. An important consequence of this bending and Li coordination is weakening of the Ta–O bonds, probably due to a decrease of Ta–O π interactions. In fact, the Ta–O distances of 4 (2.013 (6) and 2.003 (6) Å) are evidently longer than is observed for $[Cp^*Ta(CH_3)_3]_2(\mu$-O) (1.909 (7) Å).[10] Likewise, the IR band arising from Ta–O–Ta stretching vibrations moves substantially to a lower frequency in going from $[Cp^*Ta(CH_3)_3]_2(\mu$-O) (795 cm^{-1}) to 4 (585 cm^{-1}).

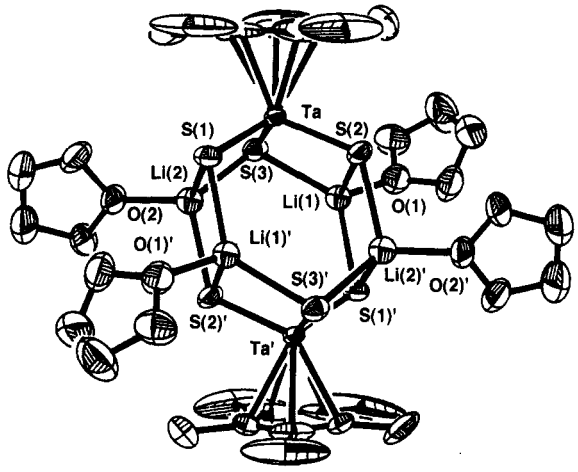

Figure 2. Molecular structure and atom-labeling scheme for $[Li_2(thf)_2Cp^*TaS_3]_2$ (**5a**) drawn with 50% thermal ellipsoids.

Table V. Selected Bond Distances (Å) and Bond Angles (deg) for $[Li_2(thf)_2Cp^*TaS_3]_2$ (5a) with Esd's in Parentheses

Ta–S(1)	2.270 (2)	S(1)–Ta–S(2)	107.1 (1)
Ta–S(2)	2.268 (3)	Ta–S(1)–Li(1a)	114.6 (4)
Ta–S(3)	2.300 (3)	Ta–S(2)–Li(2a)	127.7 (4)
S(1)–Li(1a)	2.45 (2)	S(3)–Li(1)–S(1a)	133.1 (7)
S(1)–Li(2)	2.50 (2)	Li(1)–S(3)–Li(2)	100.3 (6)
S(2)–Li(1)	2.54 (2)	S(3)–Li(2)–S(2a)	118.4 (7)
S(2)–Li(2a)	2.49 (2)		
S(3)–Li(1)	2.44 (2)		
S(3)–Li(2)	2.44 (2)		
Li(1)–O(1)	1.96 (2)		
Li(2)–O(2)	1.90 (2)		

Solid-State Structure of $[Li_2(thf)_2Cp^*TaS_3]_2$ (5a). The structure of **5a**, shown in Figure 2, is dimeric with the halves related by a crystallographic center of symmetry. Interatomic distances and angles are collected in Table V.

A striking feature of the structure is the presence of the $Cp^*TaS_3^{2-}$ unit (B). To the best of our knowledge, there is no precedent for an organometallic species having three terminal sulfides. The isolated tris(sulfido) complexes are limited to a family of inorganic MS_3E^{n-} anions (E = O, S, Se),[29,30] and for Ta the occurrence of metal–sulfur double bonds itself is very rare.[31,32] The molecule that most closely resembles B, both geometrically and electronically, is perhaps the trioxorhenium complex, Cp^*ReO_3, which also possesses a d^0 electronic configuration.[33]

The Cp^*TaS_3 portion assumes a three-legged piano-stool structure, in which the S_3 plane nearly parallels (178°) the C_5 plane of the Cp* ring. The Ta atom sits 0.92 Å

(26) Coucouvanis, D.; Hadjikyriacou, A. *Inorg. Chem.* **1987**, *26*, 1-2.
(27) (a) Setzer, W. N.; Schleyer, P. v. R. *Adv. Organomet. Chem.* **1985**, *24*, 353-451. (b) Power, P. P.; Kiaojie, Xu. *J. Chem. Soc., Chem. Commun.* **1984**, 358-359. (c) Engelhardt, L. M.; Harrowfield, J. MacB.; Lappert, M. F.; MacKinnon, I. A.; Newton, B. H.; Raston, C. L., Skelton, B. W.; White, A. H. *J. Chem. Soc., Chem. Commun.* **1986**, 846-848.
(28) (a) Tatsumi, K.; Matsubara, I.; Inoue, Y.; Nakamura, A.; Cramer, R. E.; Taogoshi, G. J.; Golen, J. A.; Gilje, J. W. *Inorg. Chem.* **1990**, *29*, 4928-4938. (b) Amstutz, R.; Seebach, D.; Seiler, P.; Achweizer, B.; Duniz, J. D. *Angew. Chem., Int. Ed. Engl.* **1980**, *19*, 53-54. (c) Weiss, E.; Joergens, U. *Chem. Ber.* **1972**, *105*, 481-486.
(29) (a) Müller, A.; Diemann, E.; Jostes, R.; Bogge, H. *Angew. Chem., Int. Ed. Engl.* **1981**, *20*, 934-955 and references therein. (b) Do, Y.; Simhon, E. D.; Holm, R. H. *Inorg. Chem.* **1985**, *24*, 4635-4642.
(30) (a) Lee, S. C.; Holm, R. H. *J. Am. Chem. Soc.* **1990**, *112*, 9654-9655. (b) Latroche, M.; Ibers, J. A. *Inorg. Chem.* **1990**, *29*, 1503-1505.
(31) (a) Drew, M. G. B.; Rice, D. A.; Williams, D. M. *J. Chem. Soc., Dalton Trans.* **1984**, 845-848. (b) Peterson, E. J.; von Dreele, R. B.; Brown, T. M. *Inorg. Chem.* **1978**, *17*, 1410-1415. (c) Sola, J.; Do, Y.; Berg, J. M.; Holm, R. H. *Inorg. Chem.* **1985**, *24*, 1706-1713.
(32) For the TaS_4^{3-} ion in extended solid structures, see ref 30b and: (a) Crevecoeur, C. *Acta Crystallogr.* **1964**, *17*, 757. (b) Omloo, W. P. F. A. M.; Jellinek, F.; Müller, A.; Diemann, E. *Z. Naturforsch.* **1970**, *25B*, 1302-1303. (c) Müller, A.; Schmidt, K. H.; Tytko, K. H.; Bouwma, J.; Jellinek, F. *Spectrochim. Acta* **1972**, *28A*, 381-391.
(33) (a) Herrmann, W. A.; Serrano, R.; Bock, H. *Angew. Chem., Int. Ed. Engl.* **1984**, *23*, 383-385. (b) Klahn-Oliva, A. H.; Sutton, D. *Organometallics* **1984**, *3*, 1313-1314. (c) Okuda, J.; Herdtweck, E.; Herrmann, W. A. *Inorg. Chem.* **1988**, *27*, 1254-1257.

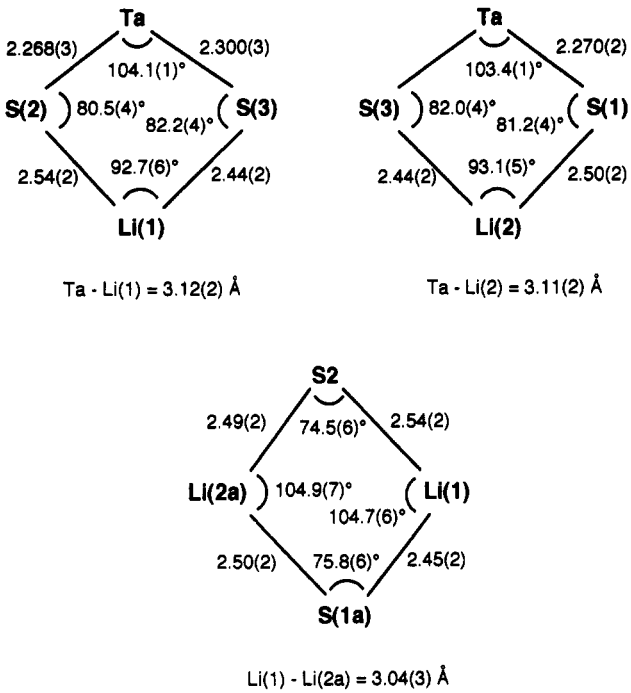

Figure 3. Bond distances and angles for the four-atom faces of the hexagonal prismatic $Li_4Ta_2S_6$ core in $[Li_2(thf)_2Cp^*TaS_3]_2$ (**5a**).

above the S_3 plane, while the Ta–Cp*(centroid) distance is 2.16 Å. The whole molecule consists of two such Cp^*TaS_3 dianions linked by four Li cations. Alternatively, the main frame may be viewed as a distorted hexagonal prism with metal atoms (Ta and Li) and sulfur atoms occupying alternate vertices. This is the third example of a prismatic M_6S_6 core, and precedents include the $Ag_4W_2S_8^{4-}$ tetraanion[34] and the $Fe_6S_6^{3+}$ portion in $[Fe_6S_6X_6]^{3-}$ (X = Cl, I, SR, OR).[35] With the structural determination of **5a**, this stereochemistry has been shown to extend to a group 1 and 5 cage and to new types of supporting ligands including the organometallic Cp* group. This also suggests that the M_6S_6 cage structure will be found in many more M_xS_y clusters.

The two six-membered rings in the hexagonal prismatic $Ta_2Li_4S_6$ cluster are not planar, but each distorts toward an approximate chair conformation. Thus the Ta and S(3a) atoms are displaced 0.71 Å down and 0.55 Å up, respectively, from the mean plane defined by S(1), S(2), Li(1a), and Li(2a) (maximum deviation, 0.009 Å). On the other hand, three crystallographically independent four-atom faces of the cluster are nearly planar, where the two $TaLiS_2$ faces have maximum deviations from the plane of 0.054 and 0.051 Å, while for the Li_2S_2 plane the maximum deviation is 0.023 Å. The dihedral angles between these faces, ideally 120°, vary from 105.4 to 135.0°.

The bond lengths and angles for these four-atom faces are shown in Figure 3. The three Ta–S bonds can be grouped into two short (2.268 (3) and 2.270 (2) Å) and one long (2.300 (3) Å) distances, albeit the differences are moderate. We will discuss the nature of Ta–S bonds in more detail later in this paper. The Li–S bond lengths range from 2.44 (2) to 2.54 (2) Å. The S(3) atom, which forms the longest bond with Ta, interacts strongly with

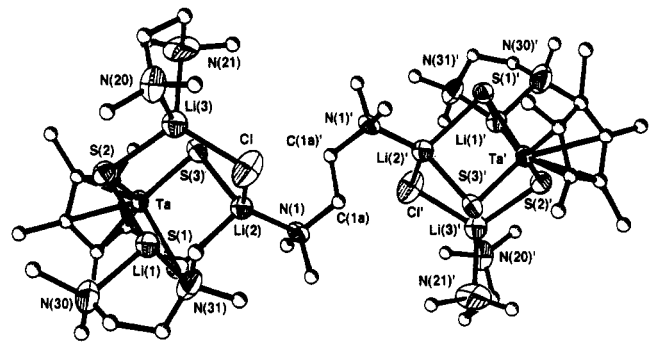

Figure 4. Molecular structure and atom-labeling scheme for $[Li_3(tmeda)_2Cp^*TaS_3Cl]_2(\mu\text{-tmeda})$ (**8**) drawn with 50% thermal ellipsoids. The right and left halves of the molecule are crystallographically related through an inversion center situated at the midpoint of the ethylene backbone of the bridging tmeda. In the structure, only the major carbon of disordered atoms, i.e., C(1a) (80% occupancy), is included.

Table VI. Selected Bond Distances (Å) and Bond Angles (deg) for $Li_3(tmeda)_2[Cp^*TaS_3Cl]_2(tmeda)$ (8) with Esd's in Parentheses

Ta–S(1)	2.298 (1)	S(1)–Ta–S(2)	102.5 (1)
Ta–S(2)	2.295 (2)	S(2)–Ta–S(3)	105.8 (1)
Ta–S(3)	2.266 (1)	S(3)–Ta–S(1)	103.3 (1)
S(1)–Li(1)	2.47 (1)	S(1)–Li(1)–S(2)	91.4 (3)
S(1)–Li(2)	2.513 (8)	S(1)–Li(2)–S(3)	92.3 (3)
S(2)–Li(1)	2.54 (1)	S(2)–Li(3)–S(3)	79.7 (3)
S(2)–Li(3)	2.509 (9)	Li(1)–S(1)–Li(2)	87.5 (3)
S(3)–Li(2)	2.447 (8)	Li(1)–S(2)–Li(3)	86.5 (3)
Cl–Li(2)	2.30 (1)	Li(2)–S(3)–Li(3)	71.6 (2)
Cl–Li(3)	2.347 (9)	S(1)–Li(1)–Cl	85.6 (3)
S(3)–Li(3)	3.118[a]	S(1)–Li(2)–Cl	116.0 (3)
Cl–Li(1)	3.445[a]	S(2)–Li(1)–Cl	85.3 (3)
Li(1)–N(30)	2.20 (1)	S(2)–Li(3)–Cl	115.4 (4)
Li(1)–N(31)	2.21 (1)	S(3)–Li(2)–Cl	104.6 (4)
Li(2)–N(1)	2.09 (1)	S(3)–Li(3)–Cl	85.6 (4)
Li(3)–N(20)	2.27 (1)	N(30)–Li(1)–N(31)	82.2 (4)
Li(3)–N(21)	2.16 (1)	N(20)–Li(3)–N(21)	83.4 (4)

[a] Nonbonding distances.

Li, so that Li(1)–S(3) and Li(2)–S(3) are the shortest Li–S distances in **5a**. There is no notable difference in Li–S bond lengths between those joining the two Cp^*TaS_3 units and those bridging within the unit. The Li–O(thf) bond lengths of 1.90 (2)–1.96 (2) Å are relatively short but fall within a normal range. Although the angles about sulfur within the four-atom faces are all accute, the shortest Li–Li distance of 3.04 (3) Å is still 0.59 Å longer than the sum of the single-bond metallic radii of 2.45 Å.[36] Similarly, the Ta–Li distances of 3.11 (2) and 3.12 (2) Å are 0.54–0.55 Å greater than the analogously calculated value of 2.57 Å. On the basis of these facts as well as the formal s^0 and d^0 electronic configuration of Li and Ta, we do not expect any direct metal–metal interactions to be present.

Solid-State Structure of $[Li_3(tmeda)_2Cp^*TaS_3Cl]_2(\mu\text{-tmeda})$ (8). The molecular structure of 8 is shown in Figure 4. The C(1a)–C(1a)′ bond lies on a crystallographic inversion center so that the halves of the molecule are identical. Selected bond distances and angles are listed in Table VI.

It is obvious that the cluster contains a pair of the pianostool $Cp^*TaS_3^{2-}$ units, like the hexagonal prismatic structure of **5a**. However, the unique feature of 8 is that each $Cp^*TaS_3^{2-}$ unit carries three lithiums coordinating at sulfurs and one chlorine atom bridging two lithiums.

(34) Stalick, J. K.; Siedle, A. R.; Mighell, A. D.; Hubbard, C. R. *J. Am. Chem. Soc.* **1979**, *101*, 2903–2907.
(35) Kanatzidis, M. G.; Hagen, W. R.; Dunham, W. R.; Lester, R. K.; Coucouvanis, D. *J. Am. Chem. Soc.* **1985**, *107*, 953–961.
(36) Pauling, L. *The Nature of the Chemical Bond*, 3rd ed.; Cornell University Press: Ithaca, NY, 1960; pp 224, 256.

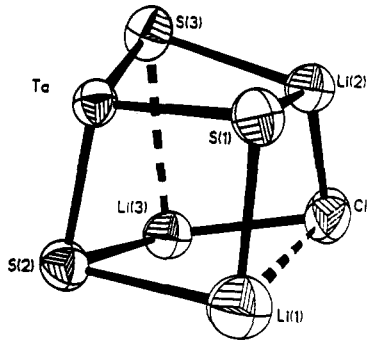

Figure 5. Perspective drawing of the open cubane Li_3TaS_3Cl core of **8** with 50% thermal ellipsoids.

The resulting two TaS_3Li_3Cl cores adopt, to a close approximation, an open-cubane geometry. Then they are linked by a tmeda ligand through interactions between two nitrogen atoms and lithiums in different open-cubane cores. In Figure 4, only the major carbon, C(1a), for the disordered methylene, is shown.

The connectivity within the Li_3TaS_3Cl core is depicted in Figure 5. Being further coordinated by tmeda ligands, all the three lithium atoms have basically tetrahedral geometries. However, their coordination environments clearly differ: Li(1) is bound to two sulfurs and two nitrogens of a chelating TMEDA; Li(2) to two sulfurs, chlorine, and one nitrogen of the bridging TMEDA; and Li(3) to one sulfur, chlorine, and two nitrogens of another chelating TMEDA. The tetrahedral coordination of the lithiums requires that two edges of the cubane be open or nonbonding. Thus Li(3)- - -S(3) (3.12 Å) and Li(1)- - -Cl (3.45 Å) are substantially longer than the sums of the corresponding covalent radii by 0.85 and 1.23 Å, respectively.[36] As a result, S(3) and Cl link only two metals.

Having metal atoms at alternate corners of the open cubane, all the metal–metal distances are long. They range from 3.05 to 3.46 Å for Ta–Li and from 3.30 to 3.46 Å for Li–Li. The Li–S distances span 2.447 (8)–2.54 (1) Å, and the shortest is understandably the Li(2)–S(3) bond. These values compare well with the Li–S distances found in **5a**. Also the observed Li–N bond distances are not aberrant.[37] Of the five crystallographically unique Li–N bonds, those associated with the two chelating TMEDA ligands are somewhat long, ranging from 2.16 (1) to 2.27 (1) Å, while the nitrogen of the bridging TMEDA coordinates at Li with a shorter Li–N distances (2.09 (1) Å).

Although the two Li–Cl bond lengths are not exactly the same, where the Li(3)–Cl bond is slightly longer than the Li(2)–Cl bond, it is not possible to specify which pair is a LiCl group. In other words, the Cl atom is tightly incorporated into the open-cubane framework, in accord with the fact that **8** does not dissociate LiCl easily from its core frame even in a polar organic solvent.

The local Cp^*TaS_3 geometry is very similar to that of **5a**. The plane defined by the five inner carbons of Cp^* is again parallel (178°) to the S_3 plane, where the displacement of Ta from these planes is 2.16 and 0.95 Å, respectively. Also the S–Ta–S angles of **5a** (103.4 (1)–107.1 (1)°) resemble those of **8** (102.5 (1)–105.8 (1)°). One notable difference can be seen in the Ta–S bond lengths. While the hexagonal prismatic structure of **5a** gives rise to two short and one long Ta–S bonds, those in the open-cubane structure of **8** are grouped into one short (2.266 (1) Å) and two long (2.295 (2) and 2.298 (1) Å) distances. As one would anticipate, the long Ta–S bonds occur with the triply bridging S(1) and S(2).

One of the more interesting features of this structure is the long, nonbonding distances along the two open edges of the cubane. What is the cause of this feature? We believe that it is a consequence of steric repulsion which occurs when the TMEDA chelates bind to the Li corners of the cubane. Let us assume for a moment that we have a closed cubane structure with each Li bound to two S and one Cl of the cube in approximate 3-fold symmetry. We then attach TMEDA chelates, which are sterically very demanding due to the two methyl groups carried by each nitrogen, to a Li ion at a corner. The chelate cannot be attached to the cube in a symmetrical fashion and one end of the chelate must be closer to one of the cubane edges than the other end. The result is that one end of the chelate finds a relatively comfortable location over one of the cube faces. The other end of the chelate, however, is then opposed to one of the cubane edges and a significant steric repulsion occurs, which results in breaking the bond along the edge of the cubane. This steric effect also lengthens the Li–N bonds. One of the Li ions, Li(2) is bound to a bridging TMEDA ligand rather than a chelating one and thus has a normal Li(2)–N(1) distance of 2.09 (1) Å. However the Li–N distances to the chelating TMEDA ligands are lengthened by the steric interaction and range from 2.16 (1) to 2.27 (1) Å. We expect that open edges caused by this type of steric effect will be the general result when chelates are attached to the metal atoms, especially if the chelate is as bulky as TMEDA.

Dynamic Solution Behavior of 8. As was mentioned earlier, the room-temperature ^1H NMR of **8** (in C_6D_6) shows a single set of TMEDA resonances. Thus, ligand-exchange processes, either between two η^2-TMEDA or between η^2-TMEDA and μ-TMEDA, occur fast with respect to the NMR time scale. This result may be relevant to the fast exchange observed between Y-coordinated DME and K-coordinated DME of $[K(\eta^2\text{-DME})_3(\eta^1\text{-DME})][Y(O\text{-}SiPh_3)_4(\eta^2\text{-DME})]$ in a CD_2Cl_2 solution, where the dynamic process was frozen at −30 °C.[38]

When the temperature is lowered, the TMEDA-based peaks for **8** in toluene-d_8 start to broaden at around 0 °C, but even at −90 °C they are not resolved. Without spectra of a slow-exchange limit, our interpretation of the fluxional behavior is limited. Nonetheless, this experiment demonstrates a very low activation energy requirement for the two TMEDA exchange processes. The unique facet of the complex **8** is that bond rearrangements within each Li_2TaS_3Cl core can in principle assist the ligand reorganization.

A mechanism for the fluxional behavior is postulated in Scheme IV, emphasizing connectivity changes in the Li_3TaS_3Cl core. The equilibration between the η^2-TMEDA ligands could be attained simply via a minor geometrical change of the open-cubane core (G ⇄ G′), and a real swap of the ligands need not to be invoked. On the other hand, the η^2-TMEDA vs μ-TMEDA equilibration requires dissociation of one η^2-TMEDA nitrogen from the tetrahedral Li center to start with, and then the other $Li_3(tmeda)_2Cp^*TaS_3Cl$ unit may shift from one terminal

(37) (a) Gregory, K.; Bremer, M.; Bauer, W.; Schleyer, P. v. R.; Lorenzer, N. P.; Kopf, J.; Weiss, E. *Organometallics* **1990**, *9*, 1485–1492 and references therein. (b) Karsch, H. H.; Zellner, K.; Müller, G. *Organometallics* **1991**, *10*, 2884–2890. (c) See also refs 18a and 27a.

(38) McGeary, M. J.; Coan, P. S.; Folting, K.; Streib, W. E.; Caulton, K. G. *Inorg. Chem.* **1991**, *30*, 1723–1735.

Scheme IV

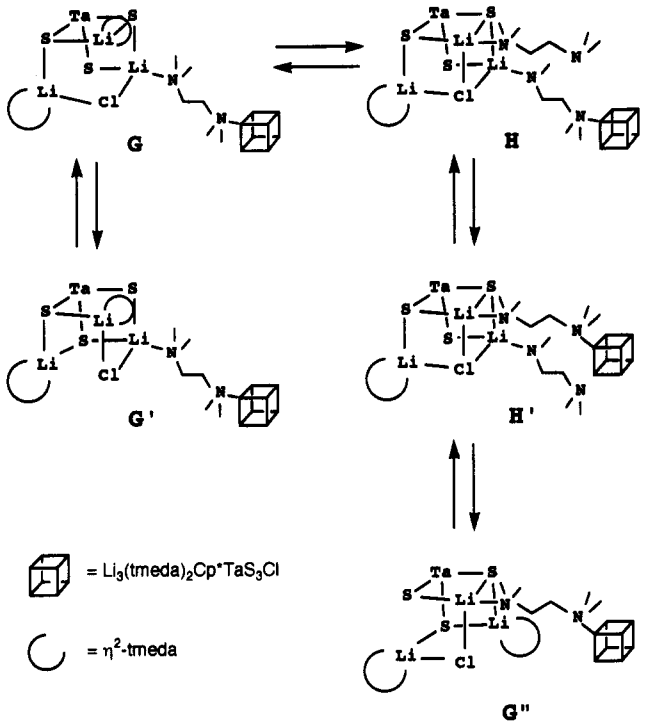

N-coordination site to the other (H ⇄ H″). Note that G, G′, and G″ are topologically equivalent, and so are H and H′. In going from G to H, partial dissociation of the η^2-TMEDA generates a vacant site at the Li center, which may be refilled by a neighboring sulfur. Thus the TMEDA arm-on/arm-off process is promoted by an S_N2 type mechanism. An important aspect of Scheme IV is that two Li_3TaS_3Cl cores of 8 can be held together during the ligand reorganization.

Remarks on Ta=S and Nb=S Bonding. Complexes **5a**, **5b**, **6**, **7**, and **8** contain the novel $Cp^*MS_3^{2-}$ unit, and the M=S bonds in this particular fragment deserve discussion.

First the Raman spectra of the closely related Ta and Nb complexes, **5a** and **5b**, are superimposed in Figure 6 (top). Their spectral patterns are remarkably similar, both of which exhibit strong bands at 434 cm^{-1} due to the M=S stretching vibrations. The result may be interpreted in two ways: (1) the observed band arises from a symmetric normal mode of the three M=S stretchings (A_1 mode for the local C_{3v} TaS_3 geometry) in which the mass effect is minimized;[39] (2) the Nb=S bonds are in fact weaker than Ta=S and the difference is apparently cancelled by the mass effect. We prefer the former explanation, because in the recently reported structures of $Li_3(tmeda)_2[MS_4]$ (M = Nb, Ta), the Nb=S bond distance of 2.274 (1) Å is even slightly shorter than Ta=S of 2.280 (2) Å,[30a] whereas the ionic radii of Ta(VI) and Nb(VI) are equal at 0.78 Å.[40] In the six- and seven-coordinate sulfide complexes of Ta and Nb, Ta=S and Nb=S distances are again not very different: $TaSCl_3(PhSCH_2CH_2SPh)$ (2.204 (5) Å)[31a] and $TaS(S_2CNEt_2)_3$ (2.181 (1) Å)[31b]; $(PPh_4)[NbS(SCH_2CH_2S)(SCH_2CH_2SCH_2CH_2S)]$ (2.192 (3) Å),[41] $NbS(SPPh_3)Cl_3$ (2.114 (4) Å), $[NbS(SPPh_3)Cl_3]_2$ (2.129 (4) Å),[42] $NbS(tht)_2Br_3$ (2.09 (8) Å), tht = tetrahydrothiophene),[43] and $NbS(S_2CNEt_2)_3$ (2.00 Å).[44]

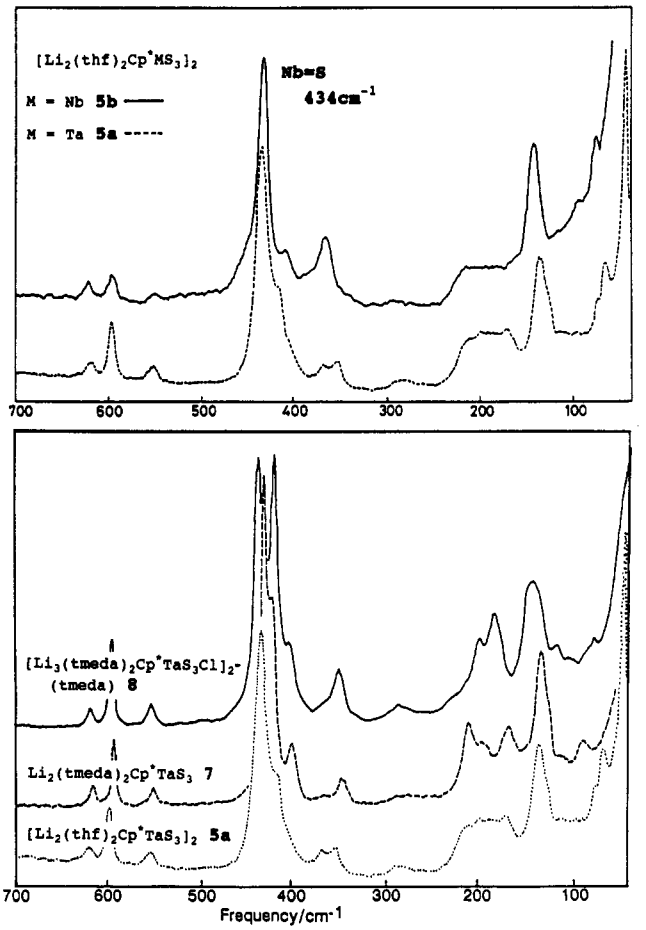

Figure 6. Comparison of the Raman spectra in the 100–700-cm^{-1} region of **5a** and **5b** (top) and **7**, **8**, and **5a** (bottom).

The Raman spectra of **6**–**8** are also similar in that they have strong bands at 432, 432, and 435 cm^{-1}, respectively. A notable difference was found in the spectra for **8** where the 432 cm^{-1} band accompanies an equally intense side band at 418 cm^{-1}. The spectra of **7** and **8** are compared with that of **5a** in Figure 6 (bottom). The appearance of the side band may have something to do with the one short and two long Ta=S distances found for **8**.

The X-ray-derived Ta=S bond lengths for **5a** and **8** range from 2.266 (1) to 2.300 Å, which are entirely comparable to that of the aforementioned complex $Li_3(tmeda)_2[TaS_4]$.[30] And these are somewhat longer than the terminal Ta=S length of the six- and seven-coordinate monosulfide complexes described earlier and those of $(Et_4N)_4(Ta_6S_{17})$ (2.145 (5)–2.204 (4) Å).[31c] The longer Ta=S distances for **5a**, **8**, and $Li_3(tmeda)_2[TaS_4]$ have to be interpreted with caution and should not be attributed entirely to the presence of Li–S interactions, because in going from sulfide to tris(sulfide) systems M=S bonds tend to be elongated due to electronic reasons.

(39) (a) If the TaS_3 portion were in the planar D_{3h} symmetry, the mass of the central metal would not affect the corresponding A_1' mode. (b) Nakamoto, K. *Infrared Spectra of Inorganic and Coordination Compounds*; Wiley: New York, 1970.

(40) Shannon, A. D. *Acta Crystallogr.* **1976**, *32A*, 751–767.

(41) Tatsumi, K.; Sekiguchi, Y.; Nakamura, A.; Cramer, R. E.; Rupp, J. J. *J. Am. Chem. Soc.* **1986**, *108*, 1358–1359.

(42) Drew, M. G. B.; Fowles, G. W. A.; Hobson, R. J.; Rice, D. A. *Inorg. Chim. Acta* **1976**, *20*, L35–L36.

(43) Drew, M. G. B.; Rice, D. A.; Williams, D. M. *J. Chem. Soc., Dalton Trans.* **1983**, 2251–2256.

(44) Drew, M. G. B.; Rice, D. A.; Williams, D. M. *J. Chem. Soc., Dalton Trans.* **1985**, 1821–1828.

Table VII. Ta=S Overlap Populations (P), Their π Components, and Charges on Sulfur Calculated for the Model Sulfide Complexes

	P(Ta=S)	$P\pi$(Ta=S)	Q(S)
$CpTaS_3^{2-}$	0.978	0.340 (0.267)[a]	-0.970
$CpTaS_3Li_2$	0.976	0.327 (0.255)	-0.853, -0.853
	0.962	0.300 (0.240)	-0.753
TaS_4^{2-}	1.019	0.377 (0.282)	-0.922
$Li_4TaS_4^+$	1.003	0.334 (0.257)	-0.710
$TaS(H)_5^{2-}$	1.070	0.433 (0.416)	-0.670

[a] The numbers in parentheses are the contribution of Ta dπ-S pπ interactions to $P\pi$.

We have performed extended Hückel calculations on the model molecules $CpTaS_3^{2-}$, Li_2CpTaS_3, TaS_4^{3-}, $Li_4TaS_4^+$,[45] and $TaS(H)_5$. The first two molecules are models for **5a**, **6**, **7**, or **8**, and the next two are for $Li_3(tmeda)_2[TaS_4]$, while the last one represents six-coordinate sulfide complexes. Table VII summarizes the computed Ta=S overlap populations (P), their π components ($P\pi$), and charges on sulfurs (Q). The P(Ta=S) for the tris(sulfide) complex $CpTaS_3^{2-}$ is evidently smaller than that for the monosulfide model $TaS(H)_5$, and the difference comes mainly from a decrease of $P\pi$, particularly from reduction of Ta dπ-S pπ interactions. However the calculated $P\pi$ for $CpTaS_3^{2-}$ is still sufficiently large to invoke a significant Ta=S multiple-bond character. Interestingly, addition of Li cations to $CpTaS_3^{2-}$ results in a relatively small drop in P (and $P\pi$). In the case of TaS_4^{3-} and $Li_4TaS_4^+$ the situation is similar to $CpTaS_3^{2-}$ and Li_2CpTaS_3. Thus our theoretical analysis indicates that elongation of the Ta=S bonds in the $Cp^*TaS_3^{2-}$ unit and in TaS_4^{3-}, relative to those in the complexes with a single terminal sulfide, is primarily due to the presence of three or four strongly π bonding terminal sulfides and that association of Li cations at sulfides is a less important factor. According to our model calculations, $CpTaS_3^{2-}$ gives a P(Ta=S) value even smaller than that of TaS_4^{3-}. This is probably due to the high π donor capability of Cp, which hinders the sulfur-to-tantalum π donor interactions.

Another important consequence of the donor nature of Cp is the highly negative charges accumulated on the sulfur atoms of $CpTaS_3^{2-}$. Also sulfurs in TaS_4^{3-} are very negative. No wonder that these sulfurs have a propensity to bind Li cations strongly. This is probably a reason why a cation exchange of Li for organic cations such as PPh_4^+ or NR_4^+ is very difficult for **5a**, **6**, **7**, and **8** and for $Li_3(tmeda)_2[TaS_4]$.

(45) Because of the polymeric nature of $Li_3(tmeda)_2[TaS_4]$, the symmetric $Li_4TaS_4^+$ cation is a better model than the neutral Li_3TaS_4.

Supplementary Material Available: For **4** and **8**, tables of complete anisotropic and isotropic temperature factors of non-hydrogen atoms (Tables S1 and S4) and hydrogen atom parameters (Tables S2 and S5) (6 pages). Ordering information is given on any current masthead page.

OM9204402